EXPLORATION OF ION-EXCHANGED GLASS FOR SEALS APPLICATIONS

A Thesis

by

ROUSHAN GHANBARI

Submitted to the Office of Graduate Studies of
Texas A&M University
in partial fulfillment of the requirements for the degree of

MASTER OF SCIENCE

August 2011

Major Subject: Nuclear Engineering

Exploration of Ion-Exchanged Glass for Seals Applications

EXPLORATION OF ION-EXCHANGED GLASS FOR SEALS APPLICATIONS

A Thesis

by

ROUSHAN GHANBARI

Submitted to the Office of Graduate Studies of
Texas A&M University
in partial fulfillment of the requirements for the degree of

MASTER OF SCIENCE

Approved by:

Chair of Committee, William Charlton
Committee Members, Paul Nelson
Sunil Khatri
Head of Department, Raymond Juzaitis

August 2011

Major Subject: Nuclear Engineering

ABSTRACT

Exploration of Ion-Exchanged Glass for Seals Applications. (August 2011)

Roushan Ghanbari, B.S., New Mexico Institute of Mining and Technology

Chair of Advisory Committee: Dr. William Charlton

As the nuclear industry grows around the globe, it brings with it a need for more safeguards and proliferation resistant technologies. The International Atomic Energy Agency (IAEA) depends on effective containment and surveillance (C/S) technologies and methods for maintaining continuity of knowledge over nuclear assets. Tags and seals, a subset of C/S technologies, are an area where innovation has been relatively stagnant for the past fifteen years. It is necessary to investigate technologies not previously used in this field in order to defend against emerging threats and methods of defeat.

Based on a gap analysis of tags and seals currently being used by the IAEA, completed with the input of several subject matter experts, the technology selected for investigation was ion-exchanged glass. Ion-exchanged glass is relatively inexpensive, has high strength, and can be used in a variety of applications. If identical pieces of glass are exchanged under the same conditions and subjected to the same point load, the fracture patterns produced can be compared and used as a verification measure. This technology has the potential to be used in passive seal applications.

Each image was categorized depending on its fracture as a ‘3 leaf’ or ‘4 leaf’ pattern. These two populations were separately analyzed and evaluated. Several methods used to analyze the fracture patterns involve the use of image analysis software such as ImageJ and the MATLAB Control Point Selection Tool. The statistical analysis software Minitab was used to validate the use of facture pattern analysis as verification tool. The analysis yielded a 60% verified comparison for samples demonstrating a ‘3 leaf’ fracture pattern and a 78% verified comparison for samples with a ‘4 leaf’ fracture pattern. This preliminary analysis provides a strong indication of the plausibility for the use of ion-exchanged glass as a verification measure for C/S measures and specifically tags and seals.

DEDICATION

I dedicate this thesis to my family for all of their love and support, not only throughout my academic career but any endeavor I undertake. They have fostered my desire to continually pursue education in all aspects of life.

ACKNOWLEDGEMENTS

I would like to thank my committee chair, Dr. William Charlton, for his guidance and support throughout the course of this research. I would also like to thank Dr. Keith Tolk, Chris Pickett, Mark Schanfein, and Dr. Hal Undem for their invaluable insights on containment and surveillance measures.

Many thanks go to Dr. Eric Taleff at The University of Texas at Austin for the use of his laboratory space and equipment. Additionally, thanks go to Dr. Rajan Tandon for his insight a willingness to answer any question. I would like to thank Dr. Stanislav Vitha for his expertise and consultation in imaging the samples.

Finally, thanks to my friends and colleagues, and the departmental staff for making my time at Texas A&M University a great experience.

TABLE OF CONTENTS

LIST OF FIGURES

Page

LIST OF TABLES

Page

CHAPTER I

INTRODUCTION

As the nuclear industry grows around the globe, it brings with it a need for more safeguards and proliferation resistant technologies. The International Atomic Energy Agency (IAEA) depends on effective containment and surveillance (C/S) technologies and methods for maintaining continuity of knowledge over nuclear assets. [1] Tags and seals, a subset of C/S technologies, are an area where innovation has been relatively stagnant for the past fifteen years. Seals are used to maintain the integrity of monitoring enclosures, containers, or perhaps a point of entry. [2] Tags are used like barcodes, as unique identifiers to account for separate items. [2] It is necessary to investigate technologies not previously used in this field in order to defend against emerging threats and methods of defeat.

Based on a gap analysis conducted with the input of several subject matter experts, the technology selected for investigation was ion-exchanged glass. The research presented in this thesis demonstrates the ability to compare and match fracture patterns of identically ion-exchanged glass disks for verification purposes. The following section provides a background for understanding C/S measures currently used by the IAEA and how ion-exchanged glass has been previously used. Chapter I defines the objectives of this thesis and background on C/S measures for safeguards. Chapter II describes the experimental procedure for fracturing the glass samples. Chapters IV and V describe the

---

This thesis follows the style of *Nuclear Technology*.

selection of ion-exchanged glass for C/S applications. Chapter III describes the image analysis for each sample and image combinations as well as statistical data analysis. Chapter VI provides conclusions of this research and recommendations for pursuing this research and design application.

I.A. Objective

The objective of this research was to provide a basis for developing a proof-of-concept containment system that utilizes ion-exchanged glass for possible post-mortem verification. This was achieved by demonstrating that identical disks of glass can undergo the ion-exchange process under identical parameters, be subjected to the same point load, and produce fracture patterns that are similar. Demonstrating this hypothesis required obtaining ion-exchanged glass samples and fracturing them under standard loading conditions. Fracturing the samples was performed at The University of Texas at Austin. The fractures samples were analyzed and compared using ImageJ and MATLAB which are both software with image analysis capabilities.

I.B. Containment and Surveillance

Containment and surveillance (C/S) technologies are used to provide a continuity of knowledge of declared nuclear assets and activities, as part of a systems approach by the IAEA. [3] The knowledge obtained should have high confidence levels to substantiate that the activities are occurring as declared. The containment systems are an integral part of ensuring that nuclear assets are controlled and protected. Additionally, containment is used in conjunction with identification to aid in the accountancy of nuclear assets. [1]

I.B.1. Seals

A seal is a tamper indicating device designed to leave non-erasable, unambiguous evidence of entry or tampering. The purpose of a seal is not to restrict or prevent access but just record that it took place. [3] Seals are mainly used for arms control and material containment, and therefore need field verification and authentication capabilities. Seals are deployed in facilities around the world, making it desirable that inspection methods are simple and additional equipment is not required.

Seals are divided into two types: passive and active. Active seals provide real time monitoring and communication to computer systems that can be accessed remotely, revealing if the seal's integrity is compromised. Passive seals require physical inspection to reveal if the seal's integrity is compromised. Both types of seals are used by the IAEA and can be applied for periods of time ranging from hours to years. [1] Figure 1 shows the Variable Coding Seal System (VACOSS), an active seal where light is pulsed through a fibre optic loop. [1] The seal records every opening and closing and this information can be transferred to and read by a computer. Figure 2 displays a passive metallic loop seal, called CAPS, after this seal is removed it is sent back to IAEA Headquarters for verification. [1] These seals are uniquely identified by imaging random scratches on the interior surface of the seals' cap and comparing the images from the installation and removal. [1]

Figure 1. A VACOSS system shown connected to a laptop [3]

Figure 2. The CAPS metallic loop seal [3]

I.B.2. Tags

Tags are unique assigned identifiers or intrinsic features that are used for asset identification. [4] The purpose of a tag is to ensure that it is extremely difficult for an adversary to counterfeit an individual identification marker that is applied to, or inherent to an asset. The IAEA uses tags to document individual assets and ensure that unauthorized replacements are not made. The reflective particle tag is shown in Figure 3. This tag utilizes micaceous hematite suspended in an adhesive matrix and can be applied to the surface of any item needing to be identified. [4] After this tag is applied to an asset or component a reader, with at least two lighting angles, is used to illuminate the tag and capture the resulting image. [4] When the tag is inspected the same lighting angles are used and another image is recorded and compares to the initial reading.

Figure 3. A reflective particle tag applied to a circuit board component [5]

I.B.3. Shortcomings of Current Tags and Seals

The majority of tag and seal technology currently used by the IAEA is at least fifteen years old. This is due to the fact that tags and seals were considered mature technologies in the mid-1980s. Very few contributions have been made to this field since that time. This means that adversaries have had at least fifteen years to figure out how to attack, counterfeit, and possibly defeat these devices. Additionally, as many as

22,000 CAPS seals can be deployed within one year, causing cost to be one of the most prohibitive criteria for the number and type of seals deployed.[6] Therefore it is necessary to identify technologies that have not been previously used in conjunction with tag and seal development for a proof-of-concept containment application.

I.C. Ion-Exchanged Glass

The process of chemically tempering glass, or ion-exchanging glass, is accomplished by immersing the glass in a molten solution of potassium nitrate where the Na^+ ions, close to the surface in the glass are replaced buy the K^+ ions from the solution.[7, 8, 9] Figure 4 shows the process of ion-exchange. This process (ion-exchange) is thermally activated and results in the strengthening of the glass.[10] The increase in glass strength is dependent on the time and temperature at which the ion-exchange occurs.[10, 11, 12, 13]

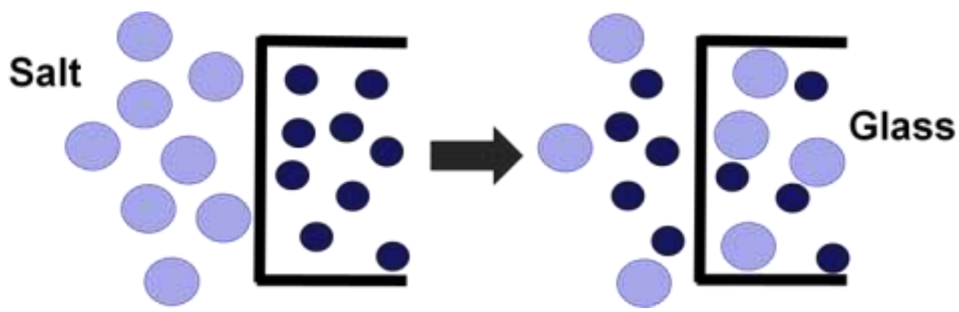

Figure 4. Schematic of the ion-exchange process, the large K^+ ions from the salt solution exchange with the Na^+ ions in the glass

In materials research several studies have been done on the fragmentation behavior of glass.[8, 11, 13, 14, 15, 16, 17] As early as 2000, investigations into ion-exchanged glass for architectural uses have been pursued. The primary motivations for these studies were to increase the strength and decrease the fragment size of glass subjected to blast environments. Using ion-exchanged glass for architectural features would mitigate the negative effects of catastrophic fracture for building occupants.[13, 14] In addition to these commercial applications, military applications where a material must serve as a barrier and subsequently be removed were examined.[8, 18] The majority of this research has come from Sandia National Laboratories in Albuquerque, New Mexico.

Several papers and presentations concerning the fragmentation of ion-exchanged glass have been published and used as guidelines for the experimental procedures of this study. At present, two papers have been published discussing the fragmentation behavior and crack branching patterns found in ion-exchanged glass; however there has been no work done trying to match the fragmentation patterns of two identical pieces of glass that were ion-exchanged under the same parameters.[11, 13]

Rajan Tandon et al[11] presents a study focused on understanding the fragmentation process of ion-exchanged glass. Tandon is particularly interested in processing conditions for ion-exchange that produce a desired combination of strength and predictable fragment size. There are many instances where reducing the size and sharpness of fragmented glass would be desired. For example, the glass shards resulting from the Oklahoma City bombing in 1995 injured more than 400 people as far as one mile away.[19]

A portion of Tandon's research focused on crack branching process and how it is affected by the ion-exchange times. Alumino-silicate (Corning Code 0317) glass disks were ion-exchanged for time intervals of 3, 6, 12, 24, 48, and 96 hours at 450 °C. Each disk was taped on one side to hold the fragments in place. [11] Each sample was subjected to an unspecified point load, on the un-taped side, applied by a Vickers diamond indenter and held for 15 s. The fragmented samples were then photographed and analyzed. The results demonstrated that an increase in exchange time caused crack branching to occur closer to the origin and decreases the fragment size distribution. Therefore in samples with long exchange times (i.e. 96 hours) the fragmentation behavior is visually indistinguishable. [11]

The work of J.E. Kooi et al [13] was based on the same exchange times and temperature, and experimental procedure as Tandon et al. Kooi's motivation was to examine how fractures propagate and determine the stresses in the glass responsible for creating crack branching patterns. The primary focus of Kooi's investigation was the correlation of the "crack branching coefficient" (CBC), a fractal dimension measure of the microscopic crack branching pattern, to the stress state of the glass prior to being fractured.

In Kooi's experiment, six sets of three glass disks (Corning 0317) were fractured using two methods, indentation and biaxial. The indentation method used a Vickers indenter to apply the load. Six sets of disks underwent ion-exchange and were fractured using a 295.2 N load, applied by a Vickers diamond indenter. Only the center portion (53 mm circle) of the fragmented disk was imaged, this was to avoid complications from edge effects.[13] The CBC and number of fragments (NOF) for each sample were determined using an Image analysis program, ImageJ. Figure 5 shows the comparison of the CBC and NOF as functions of exchange time. Both the CBC and NOF increase with exchange time, as observed by Tandon.

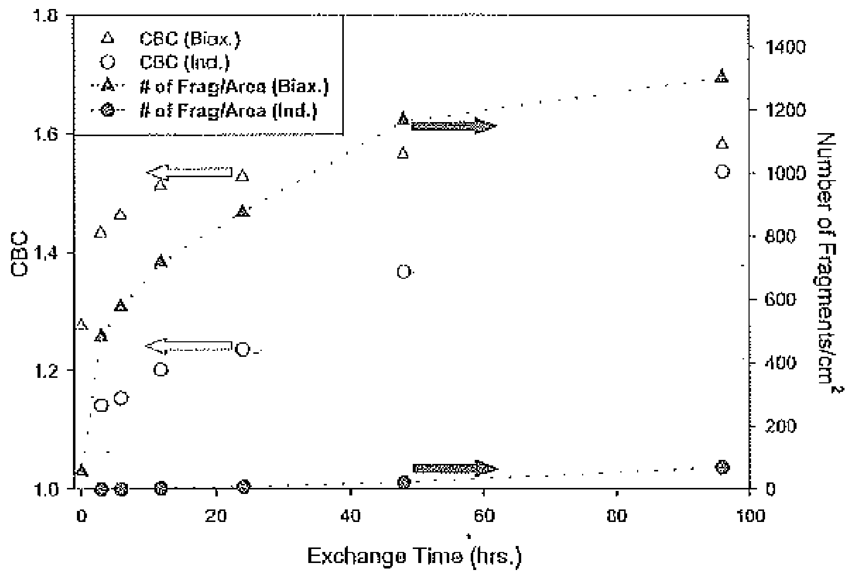

Figure 5. The CBC and NOF for indentation and biaxial fracture samples as a function of exchange time [13]

I.C.1. Current State of Ion-Exchange Technology

Currently, ion-exchanged glass is used for a variety of applications, both commercial and private. Some of these applications include cell phone screens, automobile windshields, architectural design, and military uses. This process is well developed and understood for strengthening glass and causing it to fracture into small fragments. However, further investigation into the types of fracture patterns that time and temperature variations cause, is required.

CHAPTER II

METHODOLOGY FOR ION-EXCHANGED GLASS SELECTION

Selecting a technology to be analyzed for applications in the field of seals was done using a gap analysis. The gap analysis evaluated four categories: passive seals, active seals, tags, and 'new' technologies. A gap analysis is a tool to compare the actual performance of a device to its potential performance. Primarily displayed as a matrix, a gap analysis is a simple visual representation of optimal features that are not necessarily addressed by current designs. By understanding the gaps in presently used devices, the capabilities and limitations of 'new' technologies can be evaluated for filling the gap. The tag and seal types selected for the gap analysis are all currently in use or in stages prior to being deployed. The criteria for the 'new' technologies selection included: has not been used in a current design in the field of tags and seals, have a viable application for either a new device or can be integrated into an existing device. A preliminary gap analysis was performed using an open source analysis. This was then reviewed by subject matter experts (SME's) to achieve a final gap analysis.

The desired properties of tags and seals that were assessed by the gap analysis are as follows:

- Does not need maintenance on a regular basis
- Seal can be applied without special tools
- Easy to verify seal integrity on-site
- Durability for normal wear and tear

- Training required for using seal is minimal or non-existent, this saves time and ultimately money
- Difficult to replicate
- Reusability for seals would be optimal for transfer to other assets
- Readiness level evaluates the maturity of the technology
- Security ratings speak to the components used in a seal and the methods used to evaluate its integrity
- Lifetime of a seal should be longer in case it is overlooked during an inspection
- Suitable for safeguards means that it ranks high in the previous categories, making it difficult for an adversary to defeat
- Suitable for arms verification encompasses many of the same desired traits as safeguard suitability but electronics packages and other attributes are not wanted
- Cost is one of the biggest factors, low cost is extremely important

Each technology was evaluated based on these thirteen characteristics. An 'X' denoted that the device met the requirements and a blank cell signified a gap. Research on the availability of device components and manufacturing requirements was also done when assessing each device.

The passive seals, active seals, and tags selected for evaluation are some of the most common used by the IAEA. These devices have been deployed all over the world and there is a significant amount of information lending itself to their analysis. The merits and limitations of these devices are well known and have been presented at multiple workshop and conference proceedings.

II.A. Evaluation of Gap Analysis

Four subject matter experts (SME), Dr. Keith Tolk from Sandia National Laboratories, Chris Pickett from Oak Ridge National Laboratories, Dr. Halvor Undem from Pacific Northwest National Laboratories, and Mark Schanfein from Idaho National Laboratories reviewed the analysis and provided input on optimal features and desired capabilities of tags and seals. Three of these individuals have also worked for the IAEA. In addition, the SMEs contributed insight on the rankings for each device as well as supplementary comments. Although several of the evaluation criteria are somewhat subjective (i.e. 'Security', 'Suitability for Safeguards', 'Suitability for Arms Control'), based on a series of revisions a consensus was reached, providing a complete analysis. Tables 1, 2, and 3 show the gap analysis of the passive seals, active seals, and tags, respectively.

Table 1. Gap Analysis of Passive Seals

	Metal Cable Seal	Wire Loop Seal	Adhesive Seal	Bolt-Type Seals	Shrink Wrap	Fiber Optic	Ultrasonic Sealing Bolt
Does not need Maintenance on a Regular Basis	X	X	X	X	X	X	X
Seal can be Applied without Special Tools	X	Sometimes	X	X	X	X	
Easy to Verify Seal Integrity On-Site	X	X	Not always	Not always	X	X	X
Durability for Normal Wear and Tear	X	X		X		X	X
Training Required for Using Seal					X	X	X
Difficult to Replicate						X	
Reusability						X	
Readiness Level (1-9)	9	9	9	9	9	9	9
Security (1-9)	2	5	3	5	4	8	8
Lifetime of Seal	3 years	3 years	24 hrs	1 year	3 months	5 years	4 years
Suitable for Safeguards	Low	Medium	Low	Medium	Low	High	High
Suitable for Arms Verification	Low	Medium	Low	Low	Low	High	Possibly
Cost	$	$	$	$	$$	$$$	$$

Table 2. Gap Analysis of Active Seals

	VACOSS	EOSS	IRES	TRFS	RMSA
Does not need Maintenance on a Regular Basis	Battery needs to be checked	Battery needs to be checked	Battery needs to be checked	Battery needs to be checked	Self-monitoring for battery life.
Seal can be Applied without Special Tools	Once assembled special tools are not required but to cut the cables to the appropriate length is not trivial			X	X
Easy to Verify Seal Integrity On-Site	X	X	X	X	X
Training Required for Using Seal	X	X	X	X	X
Reliability	X	X	?	X	?
Durability for Normal Wear and Tear	X	Needs more testing in the field.	?	X	?
Data Transmission Offsite	X	X	X	X	X
Data Transmission to PC Onsite	X	X	X	X	X
Data Encryption	X	X	X		X
Low Power/Battery requirements	X	X	?	X	X
Readiness Level (1-9)	9	9	8	8	8
Lifetime of Seal	2-3 years	2-3 years	?	?	?
Suitable for Safeguards	High	High	High	Medium	High
Suitable for Arms Verification	Low	Low	Low	Low	High
Cost	$$$$$	$$$$$	?	$$$	$$$

Table 3. Gap Analysis of Tags

	Image Patterns	Ultrasonic	RFID
Does not need Maintenance on a Regular Basis	X	X	X
Seal can be Applied without Special Tools	X	X	X
Easy to Verify Seal Integrity On-Site	Eyes typically are not good enough		
Durability for Normal Wear and Tear	X	X	
Training Required for Using Seal	X	X	X
Difficult to Replicate	X	X	
Reusability		X	
Readiness Level (1-9)	5 – 8	9	9
Security (1-9)	4 – 8	9	4
Lifetime of Tag	As long as records are kept	As long as records are kept	2 years
Suitable for Safeguards	High	High	Low
Suitable for Arms Verification	High	Medium	Low
Cost	$-$$$	$$$	$$

Once the analysis of the existing tags and seals, and the ‘new’ technologies were completed a determination was made between the areas for improvement and which technologies best filled these gaps. For example, if a seal was not considered difficult to replicate, what ‘new’ technology could be incorporated into the seal, making replication more difficult without compromising any of the seal’s other characteristics. Alternatively, developing a seal based on a ‘new’ technology may fill more gaps and traits from the original device could be applied to the new design concept. Upon preliminary inspection several desired capabilities and qualities were not met in each of the four categories. The passive seals technology offered no reusable seals and lower scores for security from the SME’s. Additionally, detailed and time-consuming inspection can be required to detect defeat scenarios for these seals. [20]

The analysis of active seals mainly showed limitations in the cost, making it difficult to maintain existing fulfilled requirements and consider improvements. Active seals provide high security, this is due the data encryption, verification, and authentication measures designed to thwart attacks from the State level. Battery life was the area that needed the most improvement. Extending battery life would increase the overall lifetime of the seal and therefore factor into overall cost reduction. Table 2 has several ‘?s’ under the IRES, TRFS, and RMSA categories. This is because the IRES was never fully developed and the RMSA is undergoing the last phase of testing; those performance characteristics are unknown.

Evaluating currently employed tags demonstrated the need for (in some cases simpler) on-site verification. [21] For example, not all image patterns have associated readers like the RPT and for ultrasonic tags the reader is not necessarily portable and requires verification to be done in a lab. In addition, further research was done on the finer design details of currently deployed devices since the information provided by the gap analysis was not sufficient in some instances.

The 'new' technologies being considered for tag and seal applications also extended to a variety of devices used in conjunction with tags and seals, this included considerations for better securing equipment cabinets and improved inspection methods. The preliminary eliminations of 'new' technologies were based on cost, readiness level, and security level. Table 4 shows the gap analysis of the 'new' technologies. The cost of the raw materials could not be more than three times the current cost of the least expensive, deployed system or device, the readiness level must be five or greater, and the security level must be six or greater. NASA defines technology readiness levels as "a systematic metric/measurement system that supports assessments of the maturity of a particular technology and the consistent comparison of maturity between different types of technology".[22] The "metrics" are evaluated on a scale of one to nine, where nine is the successful demonstration of a technology through standard operations. The security levels are based on a similar scale where nine is a low probability of defeating the seal without detection.

Table 4. Gap Analysis of 'New' Technologies

	Eddy Current Mapping	Eddy Current Penetration Detection	Fiber Optic Panels	IR Motion Detection	Microwave Sensors	Light Sensors	Stressed Glass	Flexible Circuit Board	Piezoelectric Film
Does not need Maintenance on a Regular Basis	X	X	X	X	X	X	X	X	X
Special Tools Required to Attach Seal	X	X	X				X	X	X
Easy to Verify Seal Integrity On-Site		High	High	Medium	Medium	Medium	High	High	Medium
Durability for Normal Wear and Tear	High	High	Medium	High	Medium	High	High	Medium	Medium
Training Required for Using Seal	Medium	Medium	Medium	Low	Low	Low	Medium	Medium	Medium
Difficult to Replicate	High	High	High	Low	Low	Low	Medium	Medium	Medium
Reusability	X	X		X	X	X	X		
Reliability	High	High	High	Medium	Medium	Medium	High	Medium	Medium
Readiness Level (0-9)	7	8	6	4	4	7	8	8	3
Security (0-9)	8	8	8	5	6	6	8	7	7
Lifetime of Technology	?	Forever	5 years	2 years	2 years	2 years	10 years	5 years	5 years
Suitable for Safeguards	High	High	High	Medium	Medium	Medium	High	High	Medium
Suitable for Arms Verification	High	Medium	High	Medium	Medium	Medium	High	High	Medium
Cost	$$$	$$	$$$$$	$$$	$$	$$	$	$$	$$

Following this approach fibre optic panels, IR motion detectors, microwave sensors, light sensors, and piezoelectric film were immediately excluded from further investigation. Fibre optic panels, while secure are exceedingly expensive especially if a replacement is needed. Several of the technologies evaluated can be spoofed by a determined adversary and have a higher probability of false alarms compared to other technologies. [23] Piezoelectric film has many desirable properties however; it has not been tested in environments similar to that in which it would be used. There is the potential that due to the possible heat and radiation effects the film would detach from a surface or deform, causing improper readings or alarms. [24] All of these technologies were intended to for use in conjunction with monitoring and securing equipment cabinets.

The next eliminations were made based on the gaps found in current devices and systems and the feasibility of filling them with the remaining technologies. Eddy current mapping has many outstanding qualities; however conducting on-site verification without a laptop and a program to compare prior and present maps is not feasible. This requires security measures needed for protecting the laptop and program from malicious attacks and directly increases the cost. [24] Eddy current penetration detection is an excellent method for ensuring the integrity of container welds or an entire enclosure. Inspecting an enclosure in its entirety can take hours depending on the size and adjusting the frequency of the current is a time consuming iterative process for defining the desired penetration depth. [25] Flexible circuit boards can be utilized in a variety of applications due to the fact that they can be easily manipulated into complex shapes.

One concern is durability, if the circuit boards were exposed to heat fluctuations or not sufficiently protected they could be damaged and need continuous repair or replacement.

The remaining 'new' technology is stressed glass; its strength, security levels, readiness levels, and availability are strong merits. It is important to note that there are two ways to stress, or temper glass: thermally and chemically. Of these two methods chemical stressing, also called ion-exchange is preferred since any shape and thickness of glass can be accommodated whereas thermal tempering is better suited for flat plates. [26] The simplicity of the ion-exchange process makes it a viable technology for a variety of applications.

Ion-exchange has become commercially available. It is used in cell phone screens, computer screens, car windshields, along with a myriad of other applications. Due to the commercial availability of this process, the majority of the expense is associated with the fabrication specifications of the glass component.

II.A.1. Application of Ion-Exchanged Glass for C/S Purposes

There are several options for using ion-exchanged glass in tag or seal applications for C/S. The simplest application is to use an initially fractured piece of glass as a tag. This would require a piece of glass to be contained, its fragmentation pattern preserved, the glass attached to an asset, and photographed. At a later date the fragmentation pattern would be inspected and compared to the originally documented pattern. For example, if the IAEA attached this tag to a piece of inspection equipment left at a facility it could be verified to be the same equipment upon return by evaluating the tag. The false alarm rate for a tag application is low, it is virtually impossible to expect two pieces of glass to produce identical fracture patterns. An adversary could attempt to recreate the fracture pattern by hand but the time needed to complete that task would likely be a deterrent.

Using ion-exchanged glass in a passive seal would be beneficial for securing the ends of a wire loop between two pieces of glass. The two ends could be sandwiched between two glass disks, of known ion-exchange parameters, and bonded by an adhesive. When the seal is removed from the asset each disk could be fractured and analyzed. This post-mortem inspection would rely on the ability to verify the fracture pattern produced by the disks and compare it to known standards for glass ion-exchanged under the same conditions.

Defeating or replicating glass for a seal application based solely on achieving the correct type of ion-exchange would be feasible for an adversary to accomplish. Ion-exchange leaves behind a chemical gradient which can be analyzed for various characteristics. In order to prevent adversaries from only having to achieve the correct ion-exchange authentication particles should be added to the glass during the manufacturing process. These particles would be similar to the micaeous hematite of the RPT, requiring the authentication of the particles prior to fracture and then verification of the fracture pattern itself. Another benefit of this additional feature is the ability to have a tag and a seal in the same device.

Attaching a glass to an asset without a flat surface would prove fairly difficult; it would be easier and more practical to utilize ion-exchanged glass in a seal application. If the verification method relied on the post-mortem fracture of the glass, analysis could be done either in the field or sent to a lab. Analyzing and verifying the fracture pattern will rely on image analysis which can easily be performed with basic equipment in a lab setting.

CHAPTER III

FRACTURE PROCEDURE OF ION-EXCHANGED GLASS

Samples of ion-exchanged glass were acquired from a commercial vendor. These samples were then fractured to assess their capability to serve as a tag and/or seal. The following sections provide detailed information on the ion-exchange of the samples and the process used to fracture the glass. Fracturing the samples takes approximately 15 s per sample. The speed and ease of this procedure is advantageous because it will reduce total verification time and total training time for performing the verification.

III.A. Ion-Exchanged Glass Sample Specifications

The glass used in this study was an alumino-silicate glass, Corning 2317, more commonly known as Gorilla® Glass. Corning no longer manufactures the 0317 glass which was used in the studies presented by Tandon and Kooi. Using the 2317 glass was an acceptable variation from the original experiments owing to the fact that 2317 has a similar composition and profile to 0317. This means that the ion-exchange process was comparable between both glasses. [27]

The 2317 glass was ordered from Marathon Glass, Stillwater, MN as a set of 20 disks, 50.8 mm in diameter and 2 mm in thickness, and underwent ion-exchange in a potassium nitrate bath for 48 hours at a temperature of 450°C. The samples were ordered to these specifications in order to minimize possible discrepancies when following the experimental procedures outlined by Tandon and Kooi. Additionally, these would be the appropriate dimensions of glass pieces to be used in the tag or seals designs mentioned in the previous chapter.

III.B. Experimental Set-up

The samples were taken to the Department of Mechanical Engineering at The University of Texas at Austin to be fractured. A Vickers macrohardness indenter (Buehler Macro Vickers 1900-2005) was tested using a HV798 hardness standard, returning a Vickers hardness value of 798.4. This reading confirming that the machine was properly calibrated. The Vickers indenter would be used to apply the appropriate load to the ion-exchanged disks, causing them to fracture. The base where the samples were fractured was wiped down to remove any debris. Figure 6, shows the experimental set-up of the equipment.

Typically a Vickers indenter is used to determine a material's hardness. However, it is particularly appropriate for this application due to the fact that a variety of loads, loading speeds, and hold times can be specified by the user. Additionally, the tip of a Vickers indenter, a square base diamond pyramid (Figure 7), allowed for easy identification of the fracture's point of initiation.

Figure 6. Experimental set-up for Vickers hardness tester

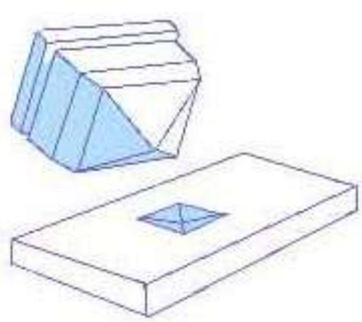

Figure 7. Square base diamond pyramid indenter and sample indentation [28]

III.C. Sample Fracturing Procedures

The samples were cleaned with acetone and transparent tape was applied to one side of each sample. The samples were marked with a felt tipped pen in the center of the disk on the taped side, shown in Figure 8. This mark was used as a reference for aligning the indenter tip with the center of the samples demonstrated in Figure 9. The samples were fractured by loading the center of the un-taped surface with the Vicker's diamond indenter with a 30 kg load, applied at a speed of 70 μm/s and held for 20 s. The tape held the sample fragments together after undergoing the indentation process.

Figure 8. Samples prior to fracture with centers marked on tape

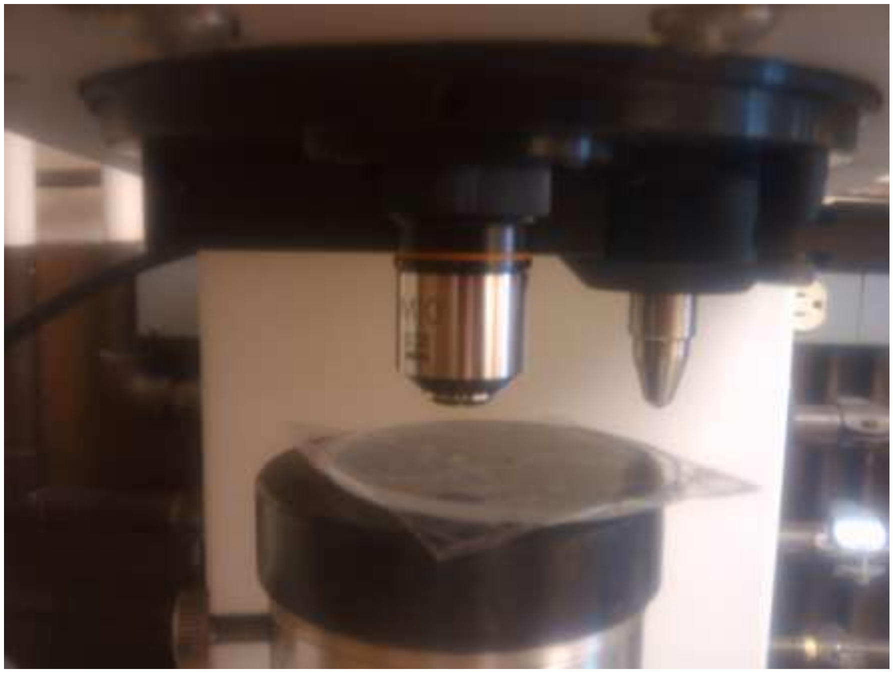

Figure 9. Sample placed on base of Vickers hardness tester prior to being fractured

CHAPTER IV

FRACTURE PATTERN IMAGE ANALYSIS

In order to verify that fracture patterns are similar, visual inspection methods are not sufficient. Image analysis software must be employed to manipulate the images and produce meaningful quantitative data.

IV.A. Visual Inspection of Fractured Samples

Upon preliminary visual inspection the fractured samples were divided into two groups, or datasets, those with a '3 leaf' fracture pattern and those with a '4 leaf' fracture pattern. Figure 10 shows a side-by-side comparison of a '3 leaf' and '4 leaf' fracture pattern. If the samples did not exhibit either of these patterns they were considered a failed sample, shown in Figure 11. One sample was lost during the fracturing process; the clear tape was not adhered to the back to ensure containment of fragments. This left 19 samples to be evaluated. Table 5 shows the fractured sample number and the respective number of leafs determined by visual inspection. Evaluating this data, based on a total of 19 samples 68.42% of samples fractured in a '4 leaf' pattern, 26.32% fractured in a '3 leaf' pattern, and 5.26% of the samples failed.

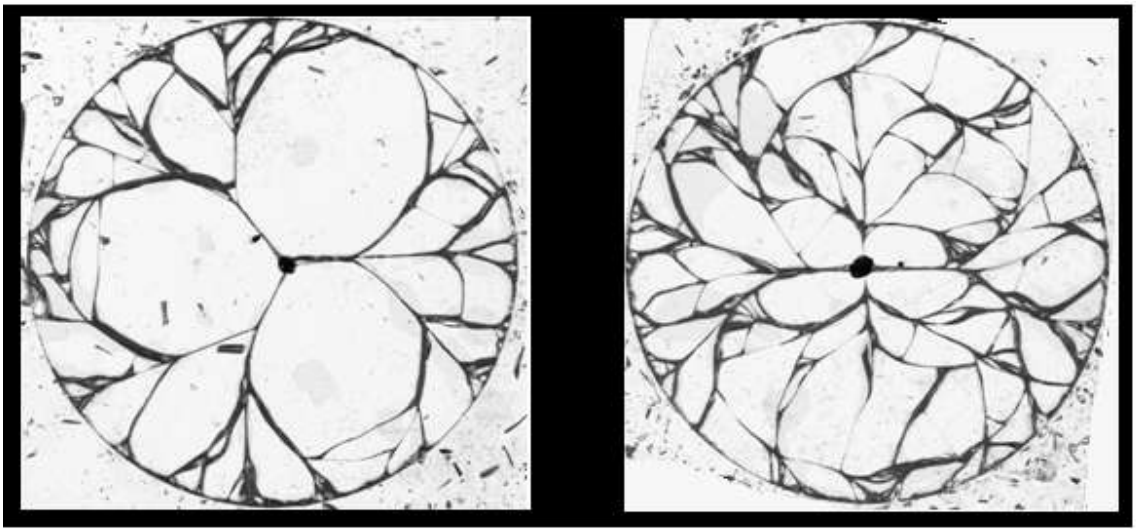

Figure 10. Scanned images of a‘3 leaf’ fracture pattern (left) compared to a ‘4 leaf’ fracture pattern (right)

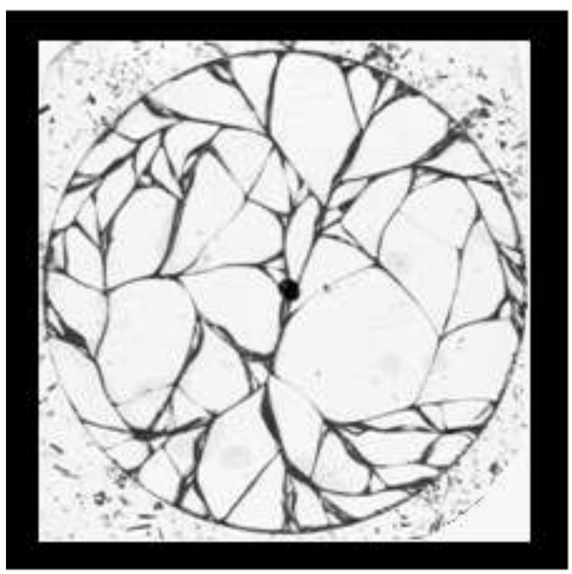

Figure 11. Scanned image of a failed sample

Table 5. Fractured Sample Number and Corresponding Number of Leafs

Sample Number	**Number of Leafs**
1	4
2	Lost
3	4
4	4
5	4
6	3
7	4
8	Failed
9	4
10	4
11	4
12	3
13	3
14	3
15	4
16	4
17	4
18	3
19	4
20	4

IV.B. Image Analysis

Images of the fractured disks were obtained through the use of a flatbed scanner (Epson Perfection 4490 Photo) and can be found in Appendix A. Each disk was placed on the scanner and scanned on the 'positive film' setting at 2400 dpi. The 19 grayscale images were converted into 8-bit images to reduce the file size and processing time for analysis. The comparisons were done on pairs of images that both have '3 leaf' patterns or images that both have '4 leaf' patterns for a total of 88 comparisons. Lookup Tables (LUTs) can be applied to one of the grayscale images to provide a better contrast when two images were combined. The LUTs apply an identity function to each grayscale pixel and replace it with preselected color, resulting in a false-color image, this result is shown in Figure 12.[29] The false-color and grayscale image combinations are used for visual inspection only. The overlay of two samples is shown in Figure 13. This method of contrasting the images allows the inspector to differentiate the fractures associated with each individual.

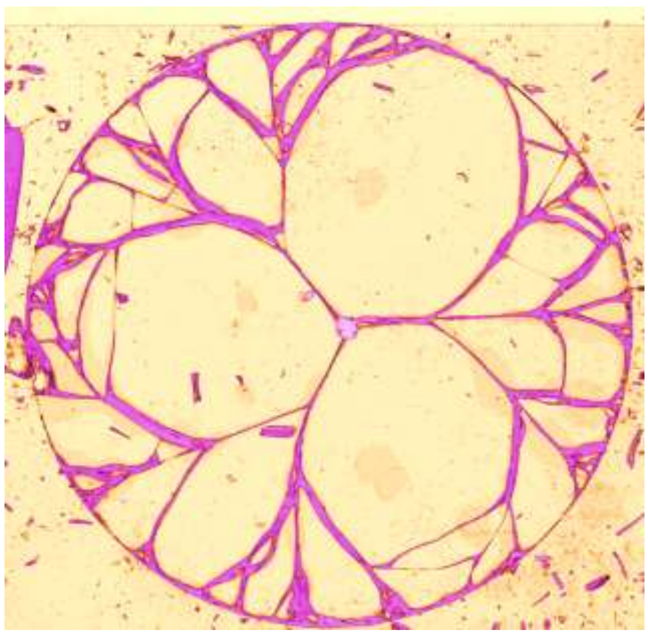

Figure 12. LUT applied to a scanned image to create a false color image

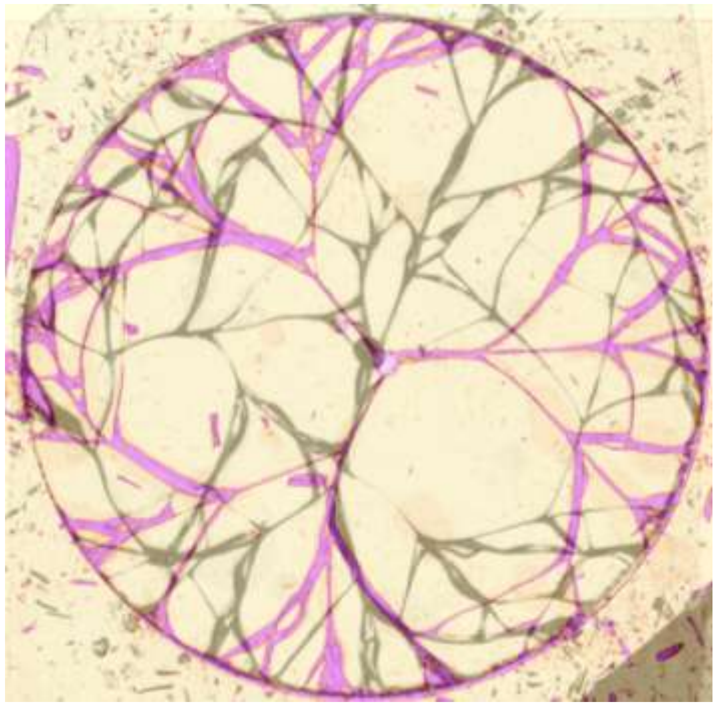

Figure 13. One sample with an applied LUT overlaid on a scanned grayscale image for visual inspection of fracture patterns

IV.B.1. Image Analysis Using the Image Processing Toolbox in MATLAB

Image analysis of the fracture patterns was performed using the Image Processing Toolbox in MATLAB. A code for image alignment and spatial transformation took advantage of the Control Point Selection Tool, allowing the user to interactively select points on a pair of images.[30] Figure 14 displays a screenshot of the Control Point Selection Tool and some of its features. To obtain the optimal alignment at least three pairs of points need to be selected, among these point should be the points of initiation and two points on the edges of each sample. In each comparison one image is defined as a 'base' image while the other is the 'unregistered' image. The 'unregistered' image will undergo the spatial transformation for the control point pairs in each image to be aligned. Once this occurs the 'unregistered' image is defined as the 'registered' image. Ultimately the 'registered' image is displayed with a semitransparent overlay of the 'base' image for comparison as seen in Figure 15. This image provides a visual reference but is not substantial for fracture pattern authentication or verification.

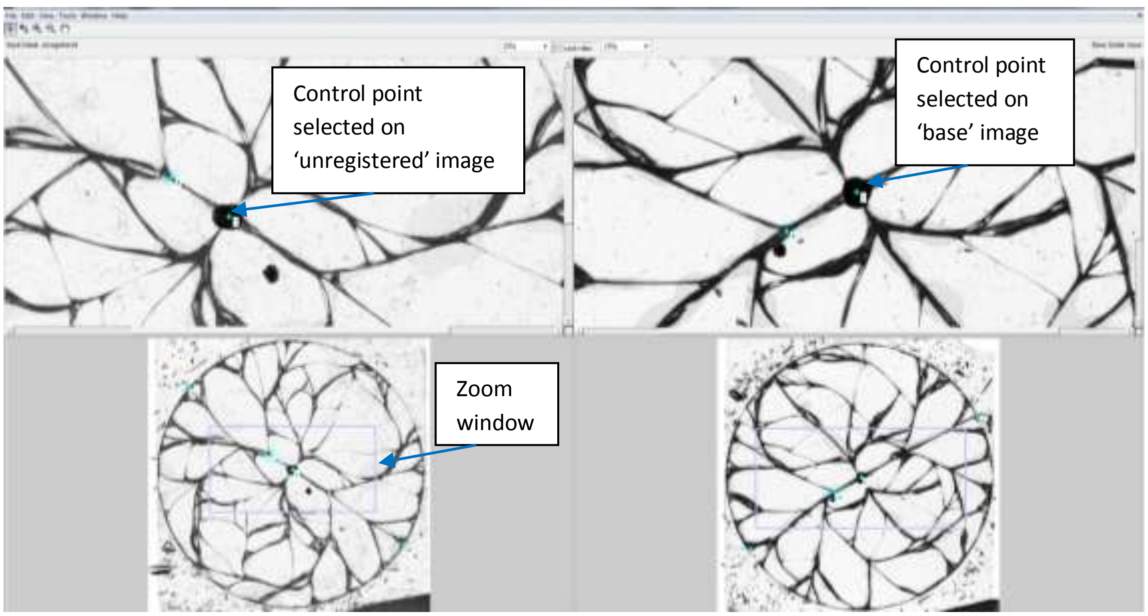

Figure 14. Control Point Selection Tool with 'unregistered' (left) and 'base' (right) images

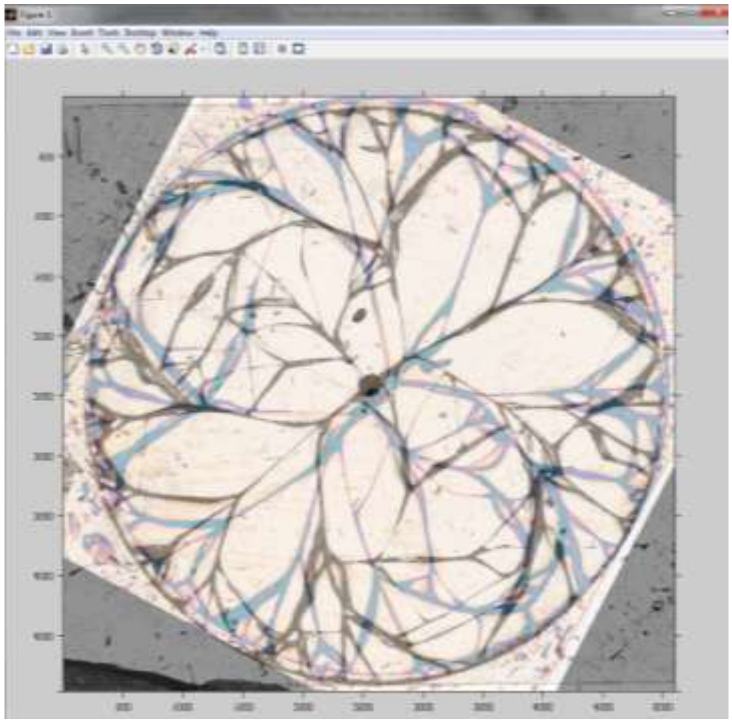

Figure 15. Semitransparent overlay of two images created using the MATLAB

IV.B.2. Image Analysis Using ImageJ

The images are also analyzed in ImageJ, an image analysis software developed by the Research Services Branch of the National Institute of Health.[31] The images can be imported from MATLAB, already overlaid, or can be manually rotated, translated, and overlaid using the Image Calculator function XOR in ImageJ. The rotation and translation of the images is achieved by the Rotate and Translate functions where the user enters in degree and pixel values, respectively. Several iterations of rotation and translation may need to be performed in order to achieve the desired alignment. Once the desired images are combined by the XOR function the resultant is converted into a binary image (cracks are displayed as black and the fragments as white). The fractures of each disk that are not matched up are displayed as black pixels, alternately where the fractures do match, the pixels are displayed. This pixel matching result is denoted by the green circles in Figure 16. Therefore, the binary image is evaluated for the percentage of black pixels in the selected area. This is achieved by defining a circular area of 0.200 inches (0.5 inch diameter) about the center of the resultant binary image. The analysis was performed on the central region of the images to avoid edge effects, where the sample underwent ion-exchange on three surfaces which produces a greater degree of fragmentation.[13] The Measure function is used to obtain the percentage of black pixels (% Area) and can provide additional information defined by the user. This process is repeated for all combinations of ‘3 leaf’ pattern images and all ‘4 leaf’ pattern images. In addition, this process was done for a select number of ‘3 leaf’ pattern images combined with ‘4 leaf’ pattern images to assess the mean percentage differences between the ‘3 leaf’ image combinations and the ‘4 leaf’ image combinations.

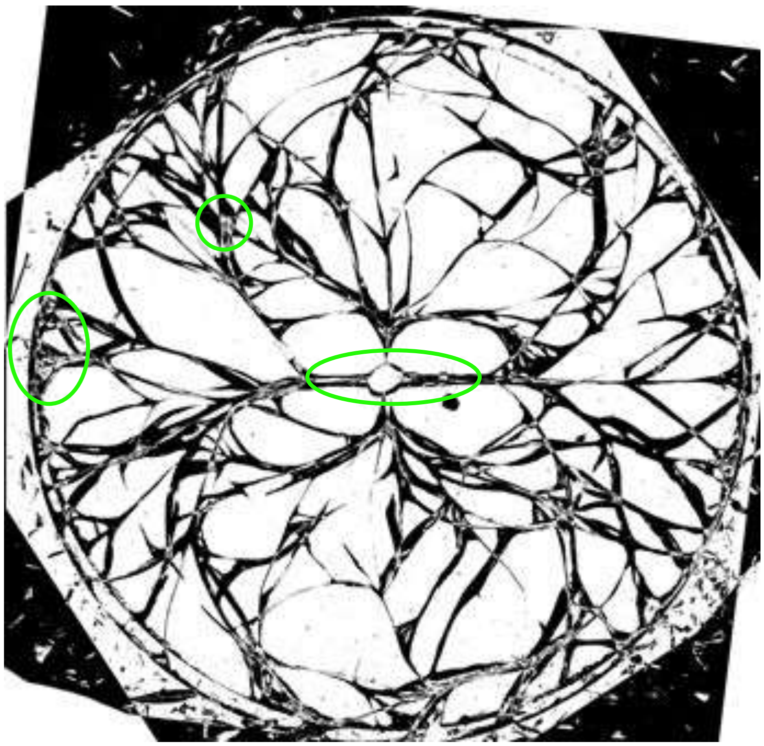

Figure 16. Binary, composite image of samples 5 and 7

CHAPTER V

RESULTS AND DISCUSSION

Presented here are the results from evaluating the fracture pattern image analysis. The discussion focuses on the statistical analysis of the fracture patterns and the composite images. Additionally, population sampling for both datasets was used to validate the use of fracture pattern analysis in deployed devices.

V.A. Statistical Analysis of Fracture Pattern Images

A total of 10 '3 leaf' composite images and 78 '4 leaf' composite images were analyzed. Tables 6 and 7 show several selected composite images and % Area for the '3 leaf' and '4 leaf' datasets, respectively. XOR denotes the ImageJ function that was used and the number following the underscores indicate the sample numbers that were combined. The complete combination of images and % Areas can be found in Appendix B. The % Area mean for the '3 leaf' combinations is 16.181%. By visual inspection of the table it is not evident that there is any one outlier from the sample group. None of the images demonstrate % Areas significantly and consistently higher or lower than the mean. The % Area mean for the '4 leaf' combinations is 20.466%. By visual inspection of the table no combinations identify a particular sample as an obvious outlier, showing % Areas significantly or consistently higher or lower than the mean.

Table 6. '3 Leaf' Composite Image Comparison Data

Image	% Area
XOR_6_12	19.373%
XOR_12_18	19.865%
XOR_13_14	11.037%
XOR_13_18	16.524%
XOR_14_18	15.723%

Table 7. '4 Leaf' Composite Image Comparison Data

Image	% Area
XOR_1_17	12.123%
XOR_3_4	24.784%
XOR_3_20	26.713%
XOR_4_11	17.011%
XOR_4_19	16.851%
XOR_9_20	21.040%
XOR_10_20	25.702%
XOR_11_20	18.412%
XOR_15_19	14.248%
XOR_16_19	15.046%

Basic statistical analysis, using the software Minitab, was done on the fractured samples. Probability plots, histograms, and other data characterizations were produced for both the '3 leaf' and '4 leaf' datasets. All of the values presented were calculated using a 95% confidence interval, meaning that 95% of the sample data would fall within the calculated range of values. These characterizations provide a sound basis for deducing meaning from both datasets.

The '3 leaf' dataset had a total of 5 samples, providing 10 combinations of images, the data shown in Table 8 is a summary of specific characteristics. The mean, standard deviation, and variance are common metrics used in statistical analysis; however, kurtosis and skewness are less common. Kurtosis measures the degree to which a dataset is peaked relative to the standard normal distribution and skewness is the lack of symmetry of a dataset. [32] These metrics can be visualized with a histogram of the data, Figure 17. The histogram is overlaid with the normal distribution, providing a graphical comparison of how well the dataset fits a normal distribution. This same comparison can also be seen with a probability plot, Figure 18. This plot provides a fitted distribution line (normal distribution) overlaid with data points and displays approximate 95% confidence intervals on either side. This provides a visualization tool for identifying possible outliers in the dataset.

Table 8. Statistical Characteristics of '3 Leaf' Composite Images

Mean	16.181%
Standard Deviation	2.661%
Variance	0.00071
Skewness	-0.311
Kurtosis	-0.259

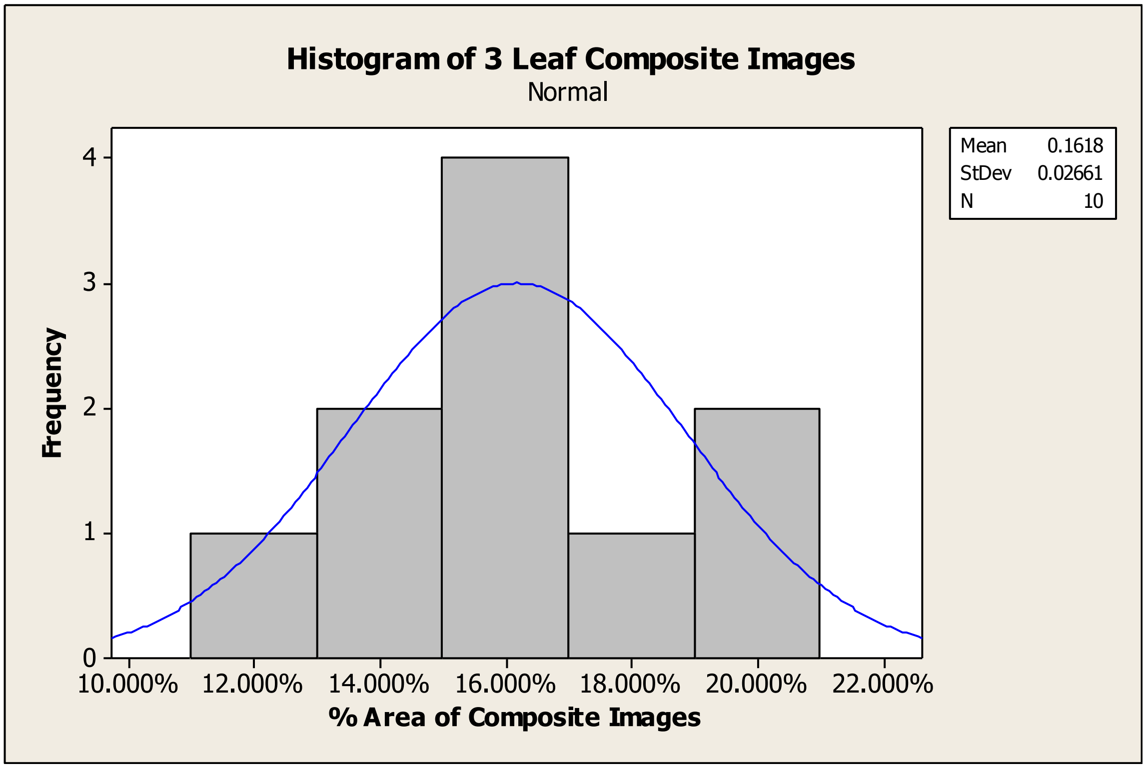

Figure 17. Histogram of ‘3 leaf’ composite images with normal fit overlay

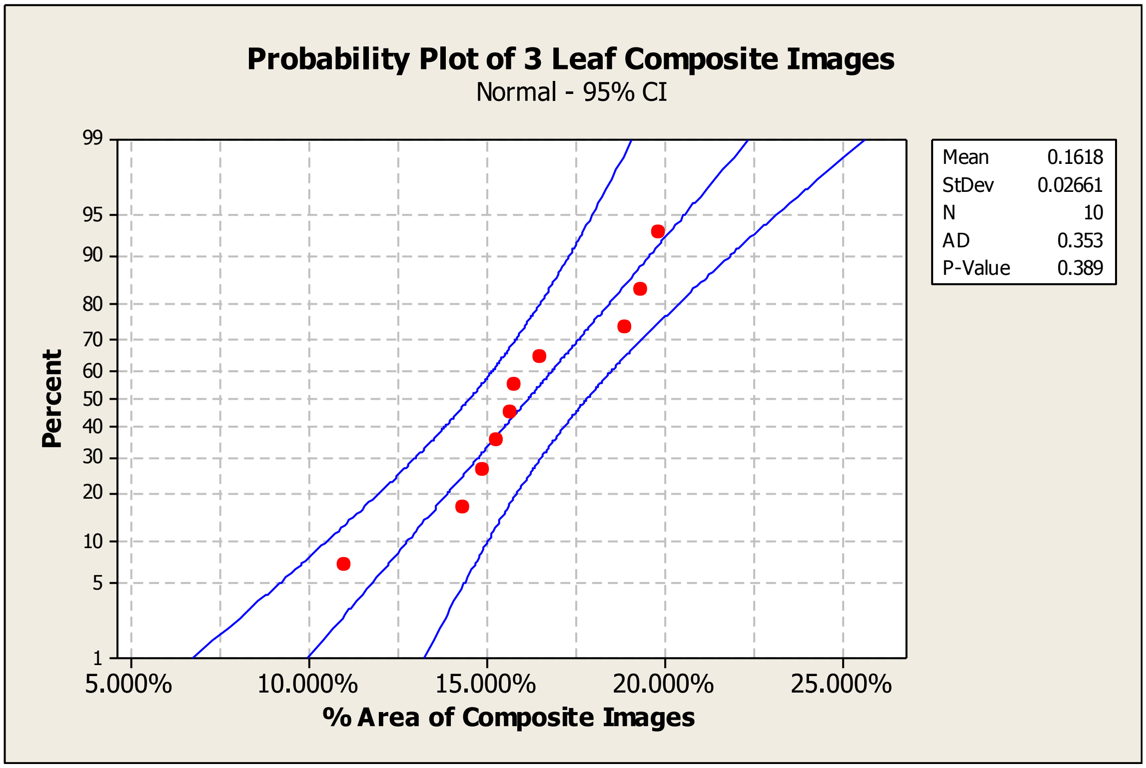

Figure 18. Probability plot of ‘3 leaf’ composite images with normal fit

The same analysis was done for the ‘4 leaf’ dataset which produced 78 combinations of images from 13 samples. The statistical characteristics are found in Table 9, while the histogram and probability plots are shown in Figures 19 and 20. It is interesting to note that both datasets have negative skewness and kurtosis values. However, with the analysis of the larger ‘4 leaf’ population the skewness is reduced. This indicates that if more samples were analyzed the data would display a greater of symmetry. It should be noted that one rule of thumb suggests if the skewness is between -0.5 and 0.5 then the distribution is approximately symmetric. [33] Following this rule, both datasets can be determined to be approximately symmetric. The negative kurtosis values demonstrated that the intermediate % Area values were more likely and the central and extreme % Area values were less likely.

Table 9. Statistical Characteristics of '4 Leaf' Composite Images

Mean	20.543%
Standard Deviation	3.448%
Variance	0.00119
Skewness	-0.251
Kurtosis	-0.695

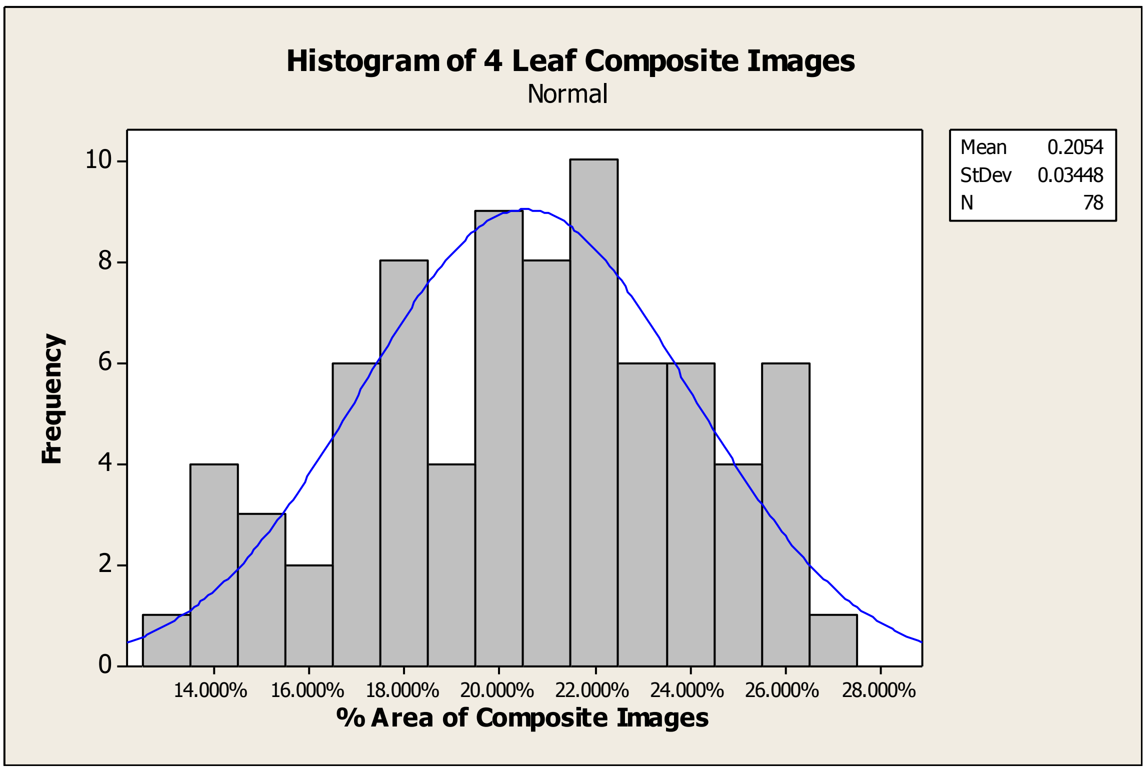

Figure 19. Histogram of '4 leaf' composite images with normal fit overlay

The standard deviations for both datasets are relatively large compared to the values of the means. It should be noted that this causes an overlap of 1.7% between the % Area averages. It is of even greater importance to note that the % Area for the '3 leaf' composite images can be contained with the distribution for the % Area of the '4 leaf' composite images. By only assessing the % Area, differentiating between a '3 leaf' and '4 leaf' fracture pattern could not be ascertained with a high level of confidence.

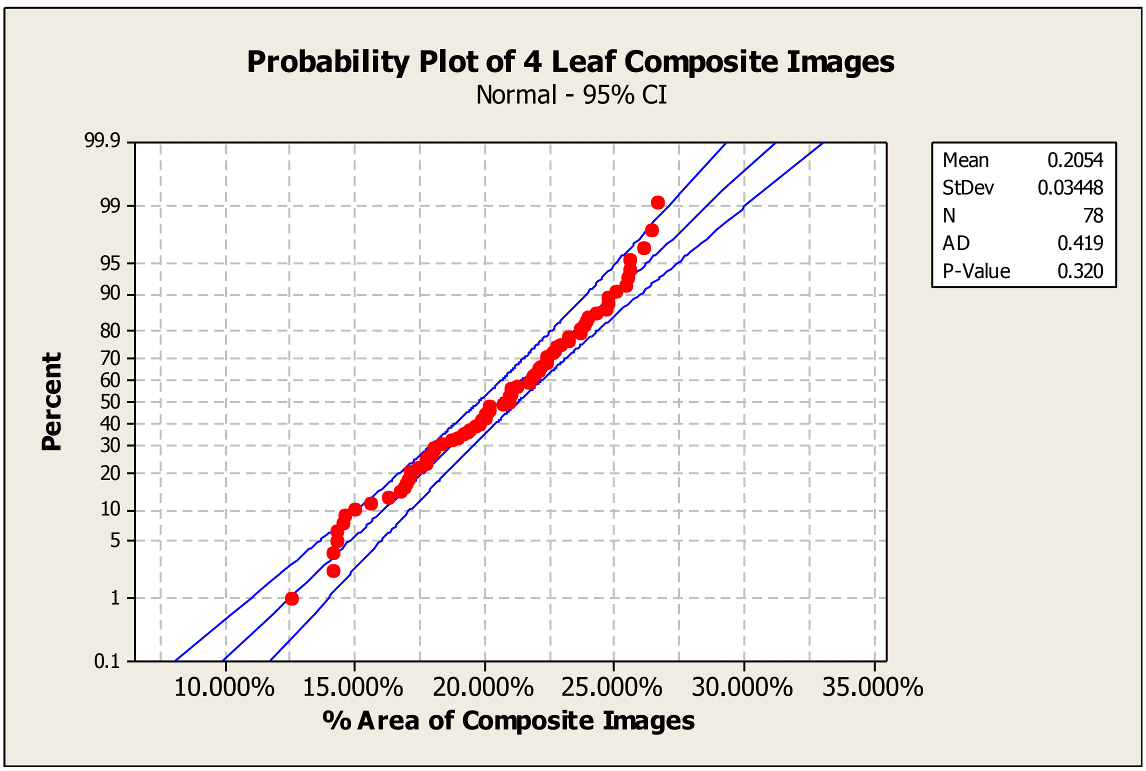

Figure 20. Probability plot of '4 leaf' composite images with normal fit

V.B. Population Sampling Analysis

It is important to simulate the post-mortem verification technique for glass seals if they are deployed in the field. One method to simulate this analysis is to select a sample from the '3 leaf' or '4 leaf' populations. This will be called the 'field' sample. The samples not selected from the respective populations will be the 'control' samples.

The composite images created with the field sample and the control samples from the respective population were analyzed. The % Area for each composite image was computed and the average calculated. Composite images of the control samples from the populations were produced for all possible remaining combinations and the % Areas calculated and averaged. This process is repeated for each sample in the respective populations, the raw data can be found in Appendix C.

The difference between the averaged % Areas of the field and control samples is calculated and compared to one standard deviation ($\pm \sigma$) of the correlating population. If the difference is less than or equal to one standard deviation the field sample is considered a match to the controls. The difference between the averaged % Areas for each field sample is shown in Tables 10 and 11 and the standard deviation and mean values can be found in Tables 8 and 9.

Table 10. % Area Difference of Field Samples for ‘3 Leaf’ Population

Field Sample	Absolute Difference
6	-1.561%
12	-1.961%
13	2.695%
14	3.447%
18	-2.621%

Table 11. % Area Difference of Field Samples for ‘4 Leaf’ Population

Field Sample	Absolute Difference
1	3.722%
3	-4.061%
4	0.797%
5	0.263%
7	-2.948%
9	0.277%
10	-3.702%
11	1.333%
15	0.945%
16	-0.943%
17	1.763%
19	3.371%
20	-1.043%

Graphical representations of the data from Tables 10 and 11 are shown in Figures 21 and 22. The samples are plotted by their % Area difference and the two red lines denote one standard deviation. The ‘3 leaf’ dataset shows a 60% pass rate, where 3 out of the 5 differences are within one standard deviation. The ‘4 leaf’ dataset shows a 78% pass rate, with 10 out of 13 calculated differences fall within one standard deviation.

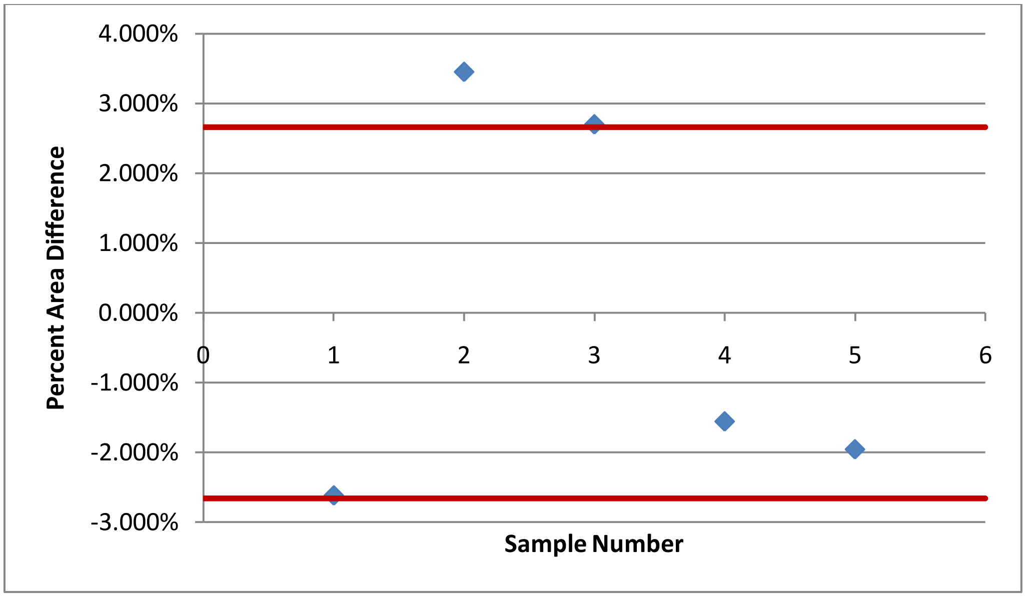

Figure 21. Comparison of '3 leaf' % area differences to one standard deviation

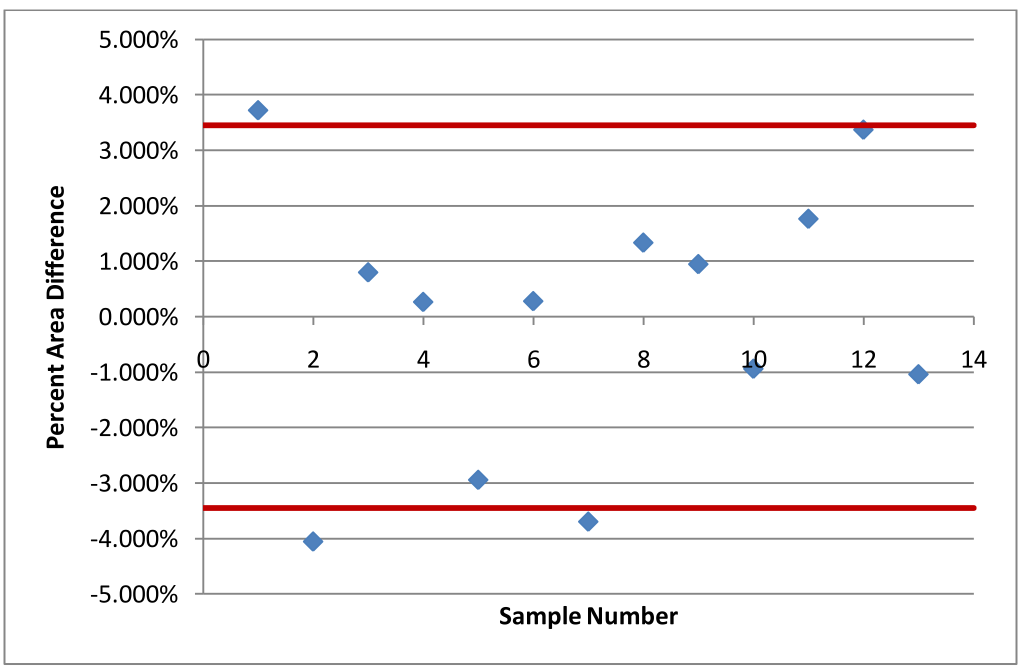

Figure 22. Comparison of '4 leaf' % area differences to one standard deviation

Comparing select images from the ‘3 leaf’ and ‘4 leaf’ datasets, shown in Table 12, yields an average % Area of 21.962%. This value is 1.496% than the ‘4 leaf’ dataset mean and 5.781% greater than the ‘3 leaf’ dataset mean. However, the majority of these ‘3 leaf’ and ‘4 leaf’ composite images give values which can be found in either dataset. This indicates the necessity of using visual inspection along with % Area calculations to differentiate between fragmentation patterns.

Table 12. % Area of ‘3 Leaf’ and ‘4 Leaf’ Composite Images

Image	% Area
XOR_3_6	27.568%
XOR_5_12	26.484%
XOR_7_13	18.504%
XOR_9_14	18.383%
XOR_11_18	22.662%
XOR_15_6	23.193%
XOR_16_12	25.344%
XOR_17_13	17.317%
XOR_19_14	16.417%
XOR_20_18	23.750%

In order to use ion-exchanged glass as an effective seal technology it is clear that verification and authentication cannot be solely dependent on fracture pattern evaluation. Only relying on % Area values for fracture patterns does not provide for any tolerance between pixels to be accounted for. Additionally, the % Area values between ‘3 leaf’ and ‘4 leaf’ patterns are minimal and visual inspection is a necessary step of the image analysis process. For additional authentication purposes particles should be added to the glass matrix for identification and the facture pattern should be evaluated for verification.

V.C. Passive Seal Design Based on Experimental Findings

Based on the results of the fracture pattern analysis it is clear that ion-exchanged glass could be used in a containment application. Figure 23 presents and exploded view of what a single use passive seal could look like. It is a loop seal, where the ends of a wire are encased between two disks of ion-exchanged glass containing authentication particles. Both disks are held together with adhesive applied in between them and a metal band encircling their circumference. The metal band would be engraved with an identification number and lot number. The identification number will be used to establish that the application of the seal to a particular asset was recorded. The lot number will be associated with specific ion-exchange characteristics (i.e. time, temperature, etc.) which would relate to the fracture pattern that seal would be expected to produce upon fragmentation.

The seal would need to be assembled on-site. One the loop has been attached to the asset the adhesive between the glass disks would be applied. The metal band would then be pressed down around the circumference of both disks. The identification number and lot number would be recorded for future verification.

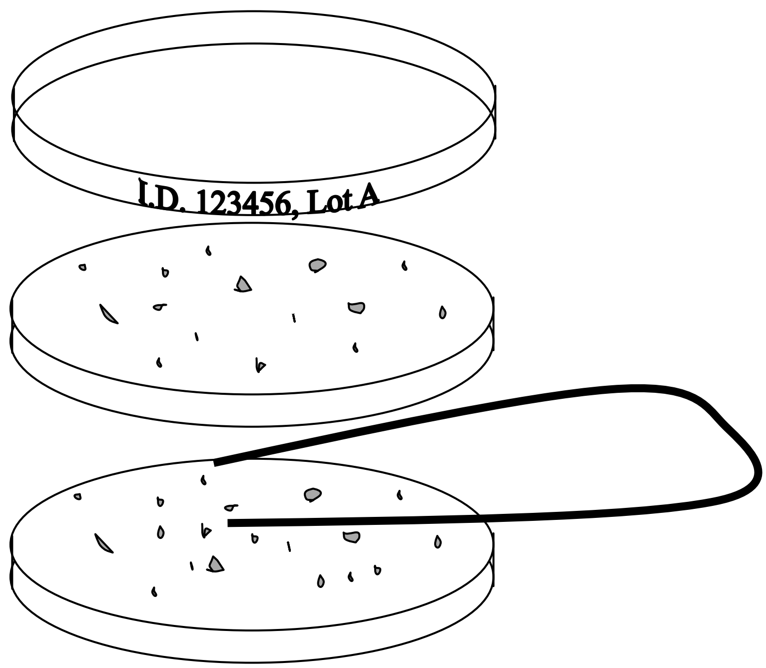

Figure 23. Ion-exchanged glass with authentication particles used in a single use, passive, loop seal

CHAPTER VI

CONCLUSIONS

Evaluating the tags and seals currently employed by the IAEA revealed several areas where improvements could be made. Increasing durability, ease of on-site verification, difficulty of replication, and decreasing cost are the primary areas of improvement for tags and passive seals, as shown in the gap analyses. Evaluating technologies not previously used in tagging and sealing applications lead to the selection of ion-exchanged glass and the optimal 'new' technology.

Identical samples of ion-exchanged alumino-silicate glass disks were subjected to an identical point load, and the fracture patterns produced were analyzed for use as a verification measure. This technology can be used for tagging and sealing devices in conjunction with existing devices or based on a standalone design. Ion-exchanged glass has many desirable characteristics such as strength, durability, and low cost for use in a tag or seals application.

Fracturing the ion-exchanged samples with a Vickers macro hardness tester provides several advantages. The primary benefit being that Vickers tester is a commercially available piece of equipment, ensuring cost remains low and availability high. Additionally, operation of a Vickers tester requires minimal training and is consistent for any material being tested.

The methodology developed for image analysis of the fracture patterns utilizes commercially available software packages and can be run on any computer supporting

Microsoft Office. This is extremely important if the verification of the fracture patterns is to be done by an individual with no specialized image analysis experience. This method is based on evaluating the resultant image from the appropriate addition and subtraction of two combined images. These predefined image arithmetic functions minimize the level of programming knowledge a user would be required to have. This is beneficial due to the fact that if fracture patterns are required to be analyzed on-site, the amount of training required in order to perform the analysis would be minimal.

The statistical analysis performed on the composite images also utilized commercially available software and provided graphical outputs for the user to evaluate the data. Based on the results of this investigation it appears that ion-exchanged glass is a viable technology for a tag or seal application. It is inexpensive, has high strength and durability, and is commercially available. A seal application requires the addition of authentication particles in conjunction with evaluating the fracture pattern for verification. Using ion-exchanged glass for a tag necessitates that the glass be fractured and imaged prior to installation and compared to its removal image. This assessment is based on the fracture patterns observed from the ion-exchanged glass samples.

Although more statistical tests need to be done pass rates of 60% for the ‘3 leaf’ and 78% for the ‘4 leaf’ datasets, for one standard deviation at a 95% confidence interval should not be discounted. Obtaining two distinct fracture patterns from identical samples may require further investigation with a larger population. If this is a common occurrence, ion-exchange parameters need extensive evaluation to mitigate obtaining the same fracture characteristics from two separately ion-exchanged batches with different characteristics. Further study necessitates another sample group that has undergone the ion-exchange process with different parameters to truly evaluate the possibility of verifying ion-exchanged glass based on distinct fracture characteristics.

In an area where new innovation has been stagnant for the past fifteen years, this research provided a proof-of-concept technology for a containment application. Ion-exchanged glass provided the desired characteristics for both tag and seal applications. Ion-exchanged glass can be used for both safeguards and arms control verification, making the development of a tag or seal dual use. Additionally, an ion-exchanged glass seal could also be designed as a tag with the addition of authentication particles. This enhancement would provide and additional function at a minimal cost. It is essential to continue the investigation of ion-exchanged glass for containment applications to provide for a safer global nuclear industry against any adversary.

CHAPTER VII

FUTURE WORK

There are several concepts presented in this research which would deserve further investigation to make an ion-exchanged seal glass a field ready; primarily the addition of authentication particles to the glass matrix during fabrication. It would be necessary to determine if the particles affect the ability to predict the fragmentation pattern of the glass. Additionally, facture patterns of various ion-exchanged batches need to be evaluated to determine specific ranges of times and temperatures that produce distinct facture patterns.

Supplementary methods of images analysis should also be examined in order to possibly compare images with a greater degree of accuracy. A two-dimensional Fourier transform could be applied to the fracture pattern images and provide a spectral analysis. [34] If the spectral components of the types of fracture patterns are unique this technique would provide an additional approach for fracture pattern analysis.

REFERENCES

1. International Atomic Energy Agency, *Safeguards Techniques and Equipment*, 2003 Edition, International Atomic Energy Agency, Vienna, Austria (2003).

2. International Atomic Energy Agency, *IAEA Safeguards Glossary*, 2001 Edition, International Atomic Energy Agency, Vienna, Austria (2002).

3. C. PICKETT and G. RICHARDSON, "Seal Selection and Performance: What Makes a Good Seal, Good," *Proc. DOD 7th Security Seals Symposium*, Santa Barbara, California February 28-March 2 (2006).

4. K. TOLK, "Random Patterns and Biometrics for Counterfeit Deterrence," SAND 93-24704, Sandia National Laboratories, Albuquerque, New Mexico (1993).

5. "Energy, Resources and Nonproliferation: Global Security," Sandia Corporation (2011); http://www.sandia.gov/ERN/global-security/capabilities.html.

6. C. MARTINEZ, Private communication, International Atomic Energy Agency, College Station, TX, March (2011).

7. D.J. MORRIS, S.B. MYERS, and R.F. COOK, "Indentation Crack Initiation in Ion-Exchanged Aluminosilicate Glass," *Journal of Materials Science*, **39**, 2399-2410 (2004).

8. S.J. GLASS, K. SCHWING, M. WARREN, and A. TAPPAN, "Stressed Glass Technology for Actuators and Removable Barrier Applications," SAND2007-4106, Sandia National Laboratories, Albuquerque, New Mexico (2007).

9. F. REHOUMA and K.E. AIADI, "Glasses for Ion-Exchange Technology," *International Journal of Communications*, **1**, 148-155 (2008).

10. R. GY, "Ion Exchange for Glass Strengthening," *Materials Science and Engineering*: B, **149**, 159-165 (2008).

11. R. TANDON and S.J. GLASS, "Controlling the Fragmentation Behavior of Stressed Glass," *Fracture Mechanics of Ceramics*, **14**, 77-91 (2005).

12. R. GARDON, "Strong Glass," *Journal of Non-Crystalline Solids*, **73**, 233-246 (1985).

13. J.E. KOOI, R. TANDON, S.J. GLASS, and J.J. MECHOLSKY, “Analysis of Macroscopic Crack Branching Patterns in Chemically Strengthened Glass,” *Journal of Materials Research*, **23**, 214-225 (2008).

14. S.J. GLASS, M. ABRAMS, and R.V. MATALUCCI, “New Glass Technologies for Enhanced Architectural Surety: Engineered Stress Profile (ESP) for Soda-Lime-Silica Glass,” SAND2000-3001, Sandia National Laboratories, Albuquerque, New Mexico (2000).

15. R.C. BRADT, “The Fractography and Crack Patterns of Broken Glass,” *Journal of Failure Analysis and Prevention*, **11**, 79-96 (2011).

16. S.J. GLASS, R. TANDON, A. VARSHNEYE, and I. SPINELLI, “Processing and Properties of Ion Exchanged Glass,” *2004 Glass and Optical Materials Division Fall Meeting*, Cape Canaveral, FL November 7-12 (2004).

17. D.J. GREEN, R. TANDON, and V.M. SGLAVO, “Crack Arrest and Multiple Cracking in Glass Through the Use of Designed Residual Stress Profiles,” *Science*, **283**, 5406 (1999).

18. M.M.A. El LEIL, F.A. CAMARATTA, and R.R. DIGENOVA, “Impact Fracture of Chemically Tempered Glass Helicopter Windshields,” *Journal of the American Ceramic Society*, **69**, 713-716 (1986).

19. S. MALLONEE, S. SHARIAT, G. STENNIES, R. WAXWEILER, D. HOGAN, and F. JORDAN, “Physical Injuries and Fatalities Resulting From the Oklahoma City Bombing,” *Journal of the American Medical Association*, **276**, 382-387 (1996).

20. K. TOLK, Private communication, Sandia National Laboratories, Albuquerque, New Mexico, June (2010).

21. C. PICKETT, Private communication, Oak Ridge National Laboratories, Albuquerque, New Mexico, June (2010)

22. J.C. MANKINS, “Technology Readiness Levels,” Office of Space Access and Technology, NASA (1996); http://www.hq.nasa.gov/ office/codeq/trl/trl.pdf

23. K. TOLK, Private communication, Sandia National Laboratories, Albuquerque, New Mexico, July (2010).

24. K. TOLK, Private communication, Sandia National Laboratories, Albuquerque, New Mexico, August (2010).

25. L. DZICZKOWSKI, “A Definition of Eddy Current Penetration Depth Useful for Flaw Detection and Conductivity Measurement,” *Proceedings in Applied Mathematics and Mechanics*, **8**, 10205-10206 (2008).

26. R. TANDON, Private communication, Sandia National Laboratories, Albuquerque, New Mexico, August (2010).

27. R. TANDON, Private communication, Sandia National Laboratories, College Station, Texas, February (2011).

28. “Vickers Hardness Testing,” MatWeb LLC (2011); http://www.matweb.com/reference/vickers-hardness.aspx.

29. T. FERREIRA and W. RASBAND, *The ImageJ User Guide 1.44* (2011); http://rsbweb.nih.gov/ij/docs/user-guide.pdf.

30. “Image Processing Toolbox,” MathWorks®, (2011); http://www.mathworks.com/help/toolbox/images/.

31. M.D. ABRAMOFF, P.J. MAGALHAES, and, S.J. RAM, “Image Processing with ImageJ,” *Biophotonics International*, **11**, 36-42 (2004).

32. K. BLACK, *Business Statistics*, 5th ed., John Wiley & Sons, Hoboken, New Jersey (2008).

33. M.G. BULMER, *Principles of Statistics*, Dover, New York, (1979).

34. “Image Processing Toolbox, Fourier Transform” MathWorks®, (2011); http://www.mathworks.com/help/toolbox/images/f21-17064.html.

APPENDIX A

Original scanned images of all samples.

Sample 1

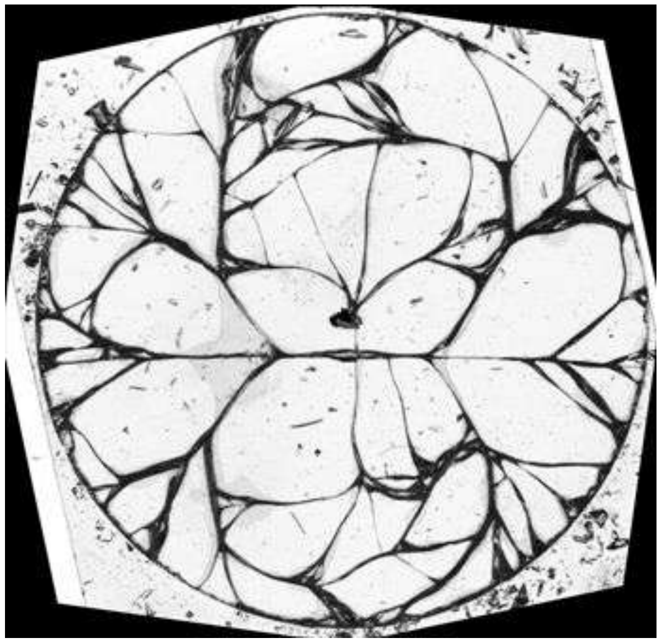

Sample 2

Sample 2 did not retain enough fragments to evaluate the fracture pattern.

Sample 3

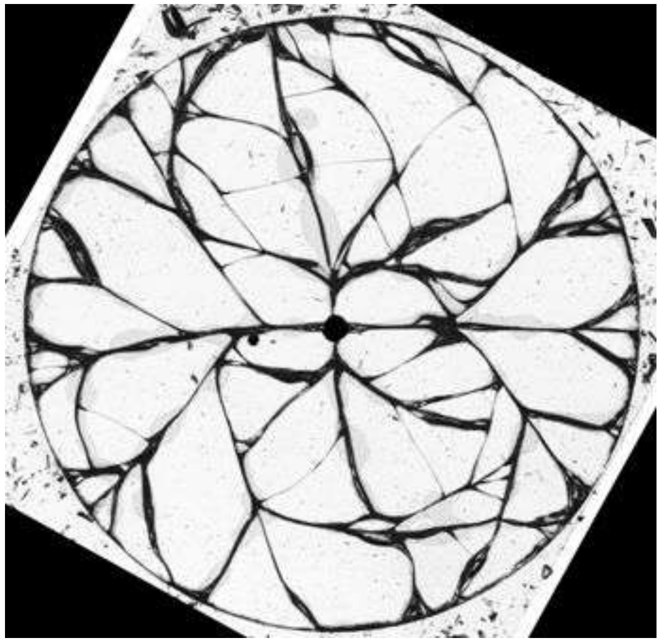

Sample 4

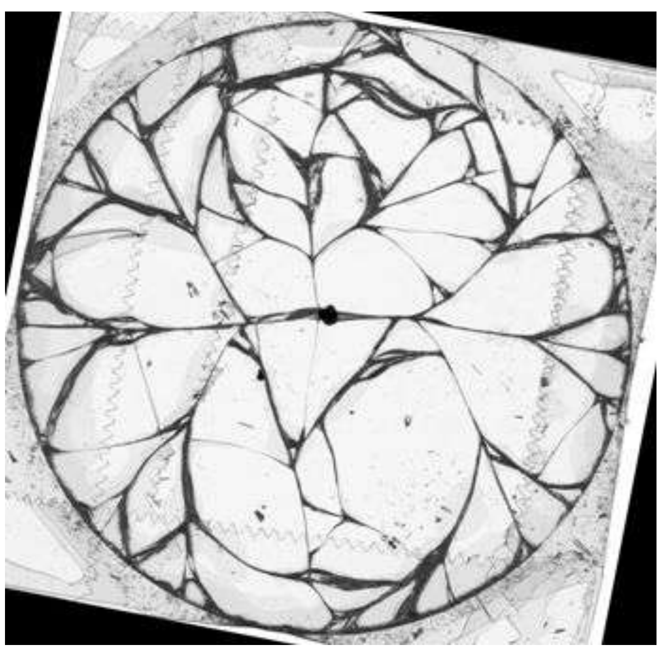

Sample 5

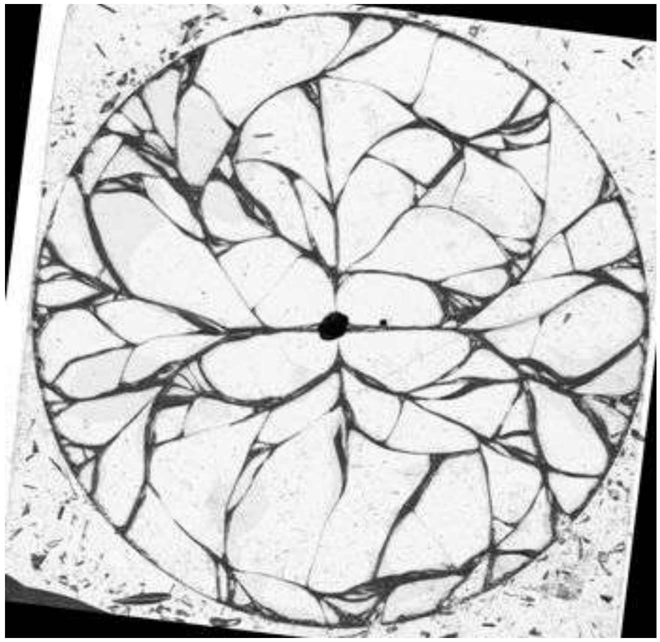

Sample 6

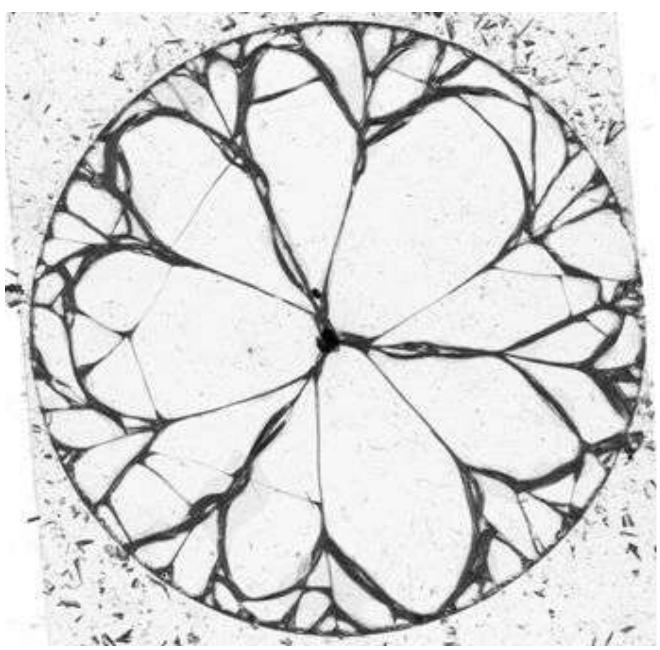

Sample 7

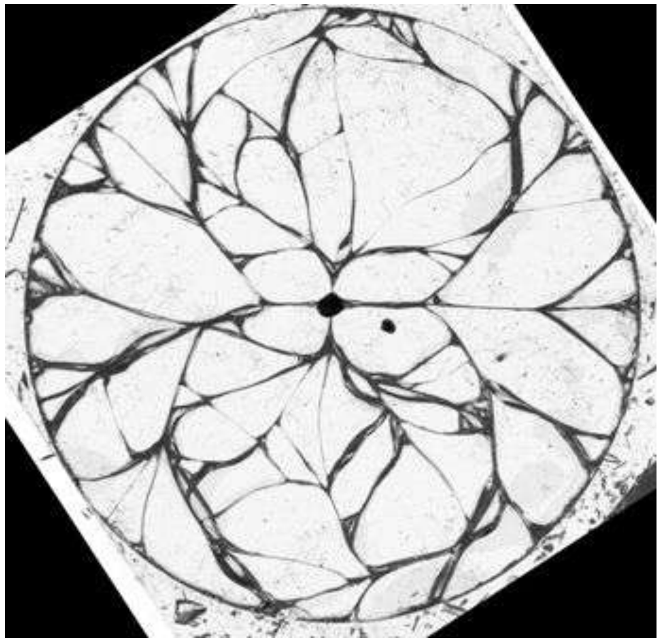

Sample 8

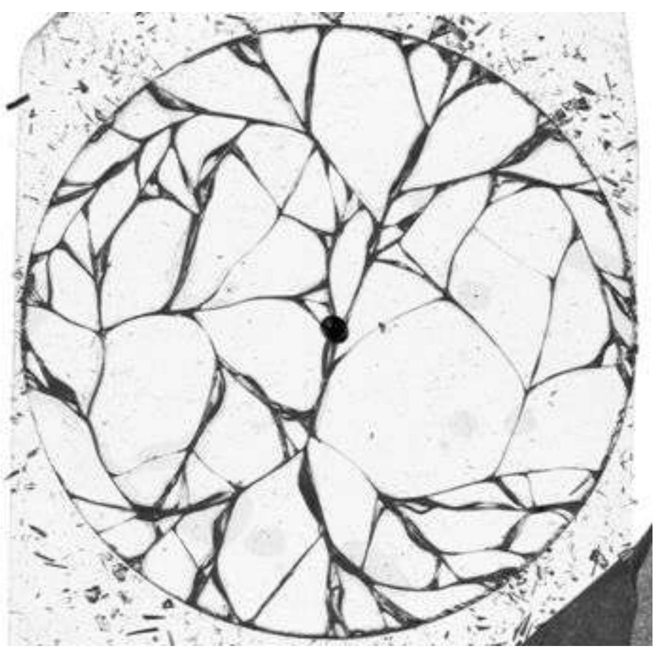

Sample 9

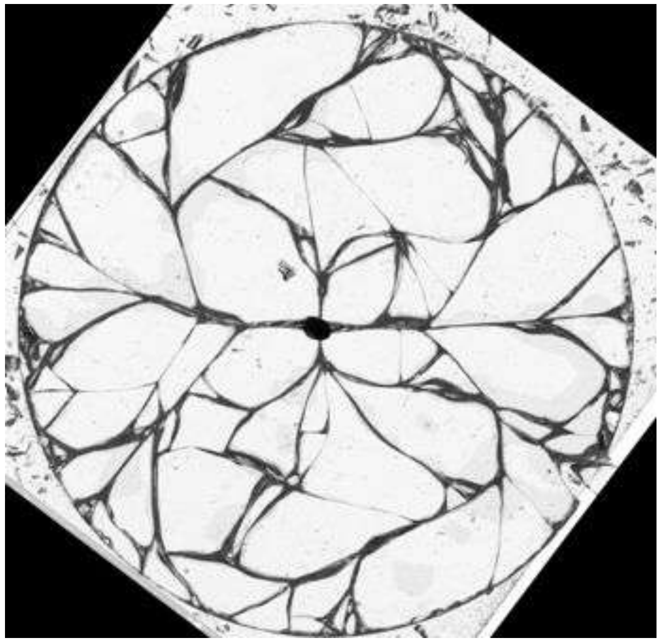

Sample 10

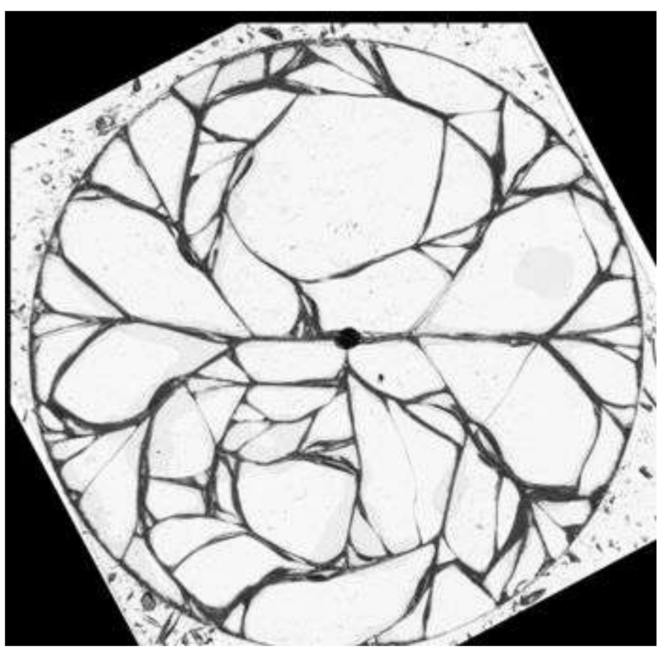

Sample 11

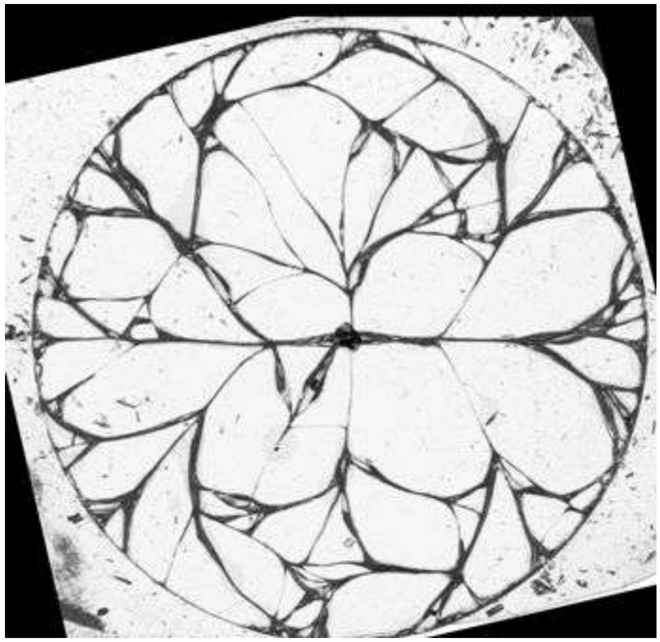

Sample 12

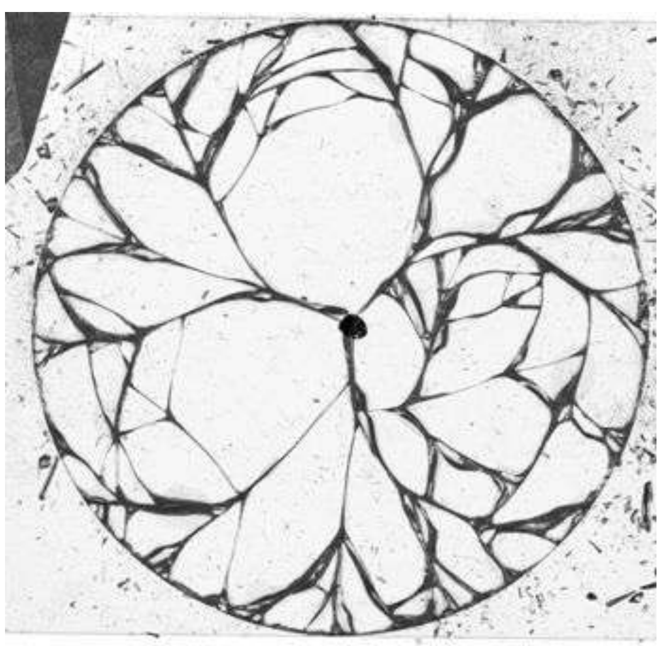

Sample 13

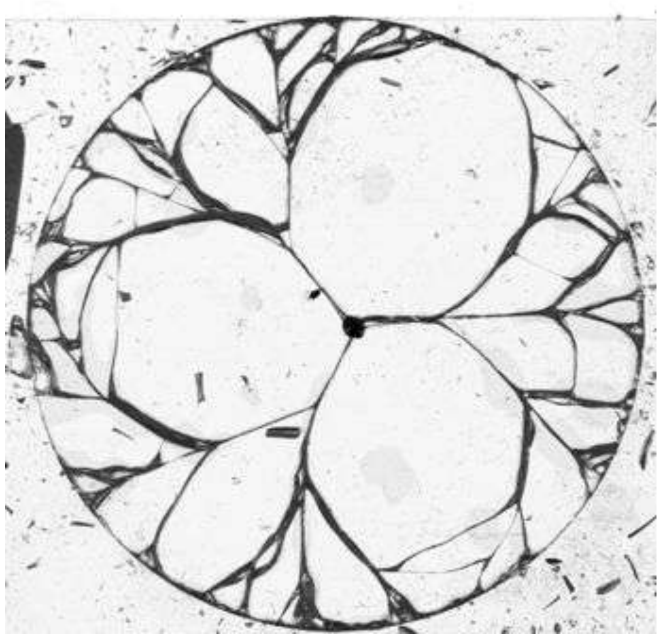

Sample 14

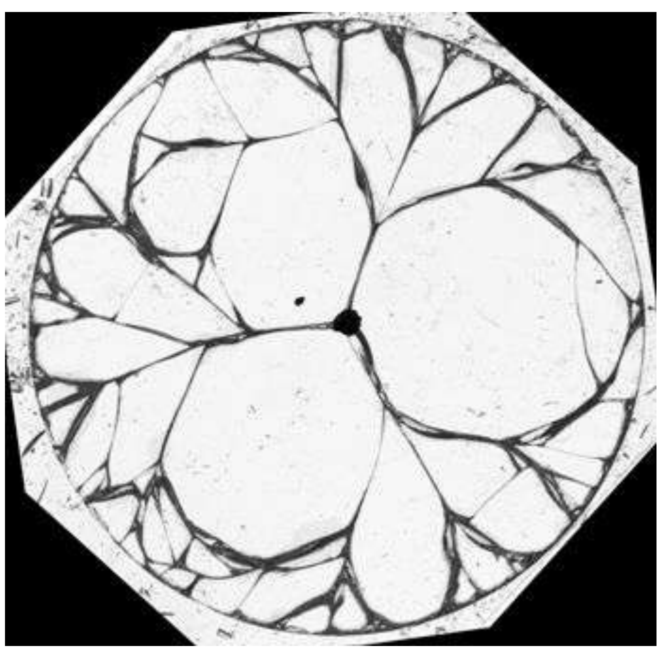

Sample 15

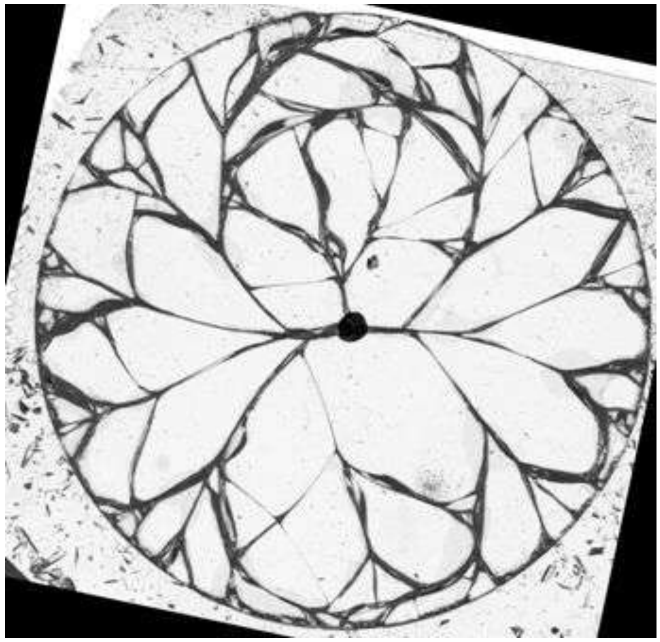

Sample 16

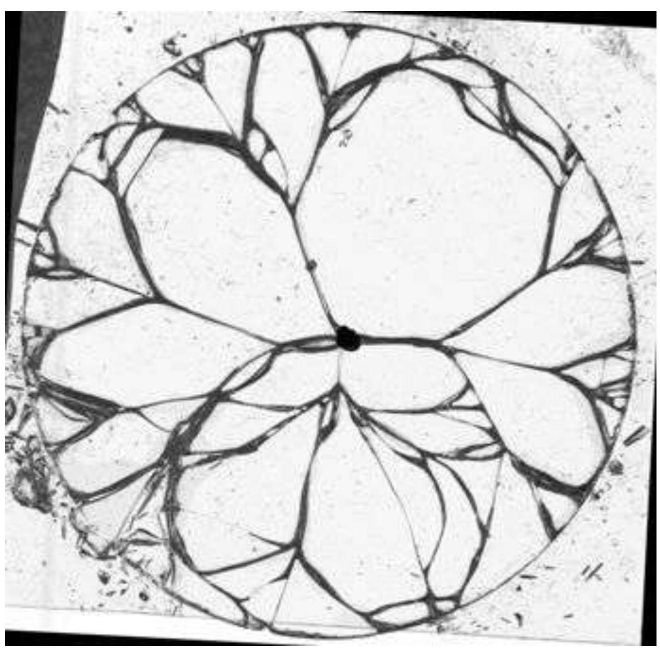

Sample 17

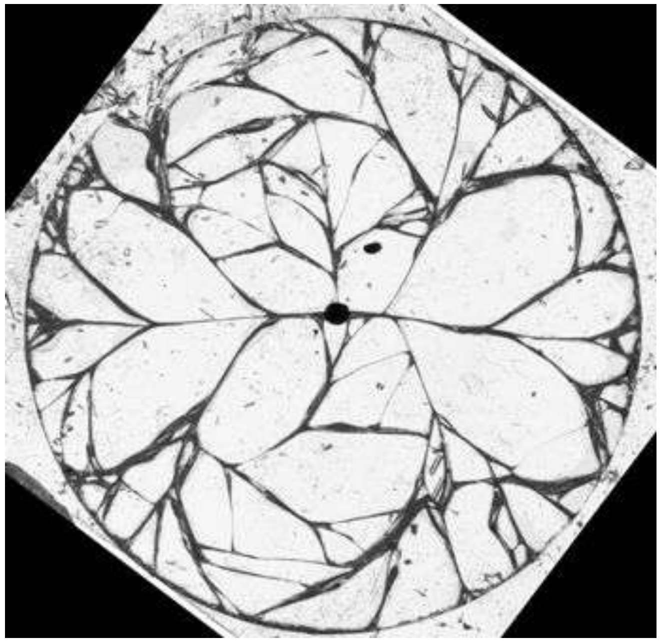

Sample 18

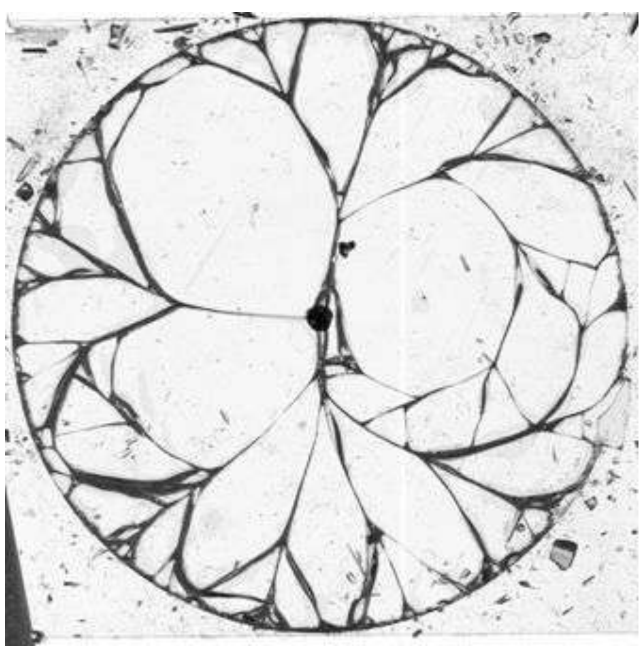

Sample 19

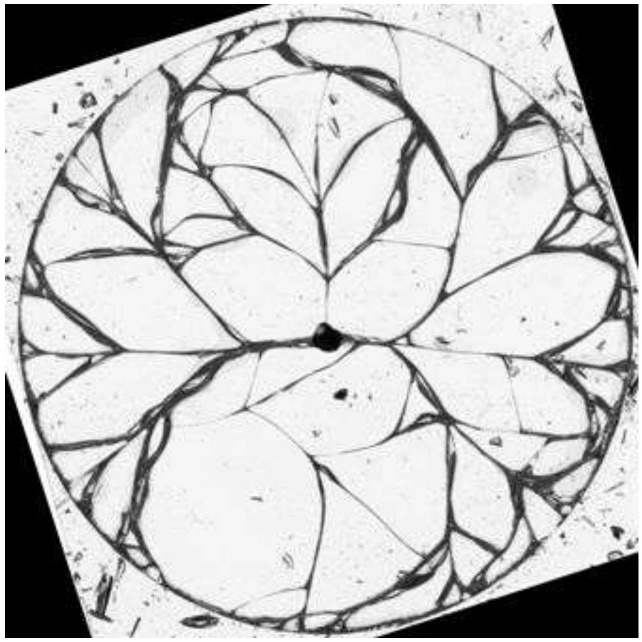

Sample 20

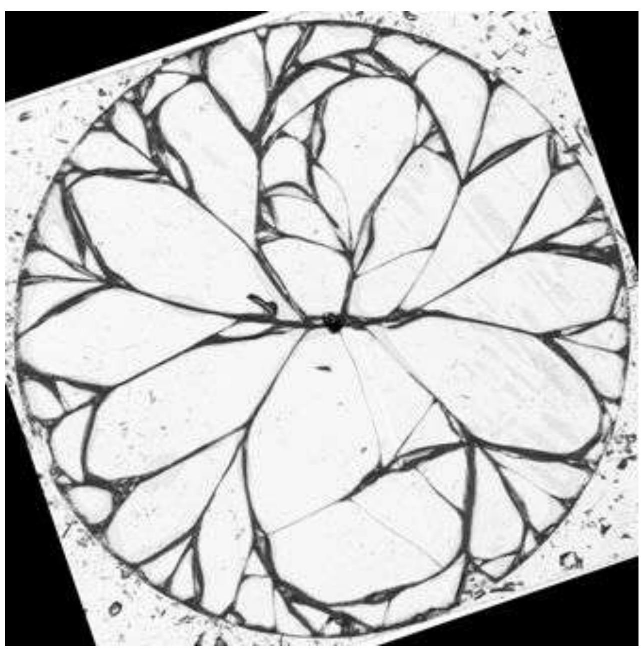

APPENDIX B

Percent of black pixels calculated in a 0.2 inch circular area taken about the center of each composite image, also called percent area (% Area). Each image is listed as the composite of two samples.

Percent Area for Composite 3 Leaf Images

Image	% Area
Composite 6 & 12	19.373%
Composite 6 & 13	14.892%
Composite 6 & 14	15.303%
Composite 6 & 18	18.903%
Composite 12 & 13	15.803%
Composite 12 & 14	14.389%
Composite 12 & 18	19.865%
Composite 13 & 14	11.037%
Composite 13 & 18	16.524%
Composite 14 & 18	15.723%

Percent Area for Composite 4 Leaf Images

Image	% Area
Composite 1 & 3	25.139%
Composite 1 & 4	16.372%
Composite 1 & 5	17.189%
Composite 1 & 7	20.766%
Composite 1 & 9	17.546%
Composite 1 & 10	22.202%
Composite 1 & 11	14.239%
Composite 1 & 15	14.602%
Composite 1 & 16	17.988%
Composite 1 & 17	12.623%
Composite 1 & 19	14.359%

Composite 1 & 20	15.696%
Composite 3 & 4	24.784%
Composite 3 & 5	20.119%
Composite 3 & 7	21.360%
Composite 3 & 9	21.834%
Composite 3 & 10	23.758%
Composite 3 & 11	22.786%
Composite 3 & 15	25.547%
Composite 3 & 16	26.219%
Composite 3 & 17	25.567%
Composite 3 & 19	23.931%
Composite 3 & 20	26.713%
Composite 4 & 5	19.302%
Composite 4 & 7	22.844%
Composite 4 & 9	20.190%
Composite 4 & 10	22.689%
Composite 4 & 11	17.011%
Composite 4 & 15	17.830%
Composite 4 & 16	20.989%
Composite 4 & 17	17.072%
Composite 4 & 19	16.851%
Composite 4 & 20	22.493%
Composite 5 & 7	23.773%
Composite 5 & 9	18.050%
Composite 5 & 10	24.411%
Composite 5 & 11	19.414%
Composite 5 & 15	20.232%
Composite 5 & 16	23.958%
Composite 5 & 17	17.793%
Composite 5 & 19	17.161%
Composite 5 & 20	22.451%
Composite 7 & 9	21.132%
Composite 7 & 10	26.480%
Composite 7 & 11	22.153%
Composite 7 & 15	23.270%
Composite 7 & 16	25.665%
Composite 7 & 17	22.224%
Composite 7 & 19	21.997%
Composite 7 & 20	24.794%

Composite 9 & 10	21.902%
Composite 9 & 11	19.725%
Composite 9 & 15	22.474%
Composite 9 & 16	21.070%
Composite 9 & 17	19.906%
Composite 9 & 19	18.836%
Composite 9 & 20	21.040%
Composite 10 & 11	24.036%
Composite 10 & 15	23.317%
Composite 10 & 16	24.808%
Composite 10 & 17	23.015%
Composite 10 & 19	21.795%
Composite 10 & 20	25.702%
Composite 11 & 15	19.927%
Composite 11 & 16	21.086%
Composite 11 & 17	19.523%
Composite 11 & 19	14.676%
Composite 11 & 20	18.412%
Composite 15 & 16	20.136%
Composite 15 & 17	18.143%
Composite 15 & 19	14.248%
Composite 15 & 20	17.201%
Composite 16 & 17	18.107%
Composite 16 & 19	15.046%
Composite 16 & 20	21.027%
Composite 17 & 19	14.391%
Composite 17 & 20	20.259%
Composite 19 & 20	19.005%

APPENDIX C

Comparison of % Area for the ‘field’ and ‘control’ samples of each dataset. Tables display the % Area of the ‘control’ sample composites in the left column and the ‘field’ sample composites are displayed in the right column.

3 Leaf Dataset

‘Control’ samples 12, 13, 14, and 18 and ‘field’ sample 6

‘Control’ Samples		**‘Field’ Sample**	
Image	**% Area**	**Image**	**% Area**
Composite 12 & 13	15.803%	Composite 6 & 12	19.373%
Composite 12 & 14	14.389%	Composite 6 & 13	14.892%
Composite 12 & 18	19.865%	Composite 6 & 14	15.303%
Composite 13 & 14	11.037%	Composite 6 & 18	18.903%
Composite 13 & 18	16.524%		
Composite 14 & 18	15.723%		

Difference between ‘control’ samples % Area and ‘field’ samples % Area, -1.561%.

‘Control’ samples 6, 13, 14, and 18 and ‘field’ sample 12

‘Control’ Samples		**‘Field’ Sample**	
Image	**% Area**	**Image**	**% Area**
Composite 6 & 13	14.892%	Composite 12 & 6	19.373%
Composite 6 & 14	15.303%	Composite 12 & 13	15.803%
Composite 6 & 18	18.903%	Composite 12 & 14	14.389%
Composite 13 & 14	11.037%	Composite 12 & 18	19.865%
Composite 13 & 18	16.524%		
Composite 14 & 18	15.723%		

Difference between ‘control’ samples % Area and ‘field’ samples % Area, -1.961%.

‘Control’ samples 6, 12, 14, and 18 and ‘field’ sample 13

‘Control’ Samples		**‘Field’ Sample**	
Image	**% Area**	**Image**	**% Area**
Composite 6 & 12	19.373%	Composite 13 & 6	14.892%
Composite 6 & 14	15.303%	Composite 13 & 12	15.803%
Composite 6 & 18	18.903%	Composite 13 & 14	11.037%
Composite 12 & 14	14.389%	Composite 13 & 18	16.524%
Composite 12 & 18	19.865%		
Composite 14 & 18	15.723%		

Difference between ‘control’ samples % Area and ‘field’ samples % Area, 2.695%.

‘Control’ samples 6, 12, 13, and 18 and ‘field’ sample 14

‘Control’ Samples		**‘Field’ Sample**	
Image	**% Area**	**Image**	**% Area**
Composite 6 & 12	19.373%	Composite 14 & 6	15.303%
Composite 6 & 13	14.892%	Composite 14 & 12	14.389%
Composite 6 & 18	18.903%	Composite 14 & 13	11.037%
Composite 12 & 13	15.803%	Composite 14 & 18	15.723%
Composite 12 & 18	19.865%		
Composite 13 & 18	16.524%		

Difference between ‘control’ samples % Area and ‘field’ samples % Area, 3.447%.

‘Control’ samples 6, 12, 13, and 14 and ‘field’ sample 18

‘Control’ Samples		**‘Field’ Sample**	
Image	**% Area**	**Image**	**% Area**
Composite 6 & 12	19.373%	Composite 18 & 6	18.903%
Composite 6 & 13	14.892%	Composite 18 & 12	19.865%
Composite 6 & 14	15.303%	Composite 18 & 13	16.524%
Composite 12 & 13	15.803%	Composite 18 & 14	15.723%
Composite 12 & 14	14.389%		
Composite 13 & 14	11.037%		

Difference between ‘control’ samples % Area and ‘field’ samples % Area, -2.621%.

4 Leaf Dataset

‘Control’ samples 3, 4, 5, 7, 9, 10, 11, 15, 16, 17, 19, 20 and ‘field’ sample 1

‘Control’ Samples		**‘Field’ Sample**	
Image	**% Area**	**Image**	**% Area**
Composite 3 & 4	24.784%	Composite 1 & 3	25.139%
Composite 3 & 5	20.119%	Composite 1 & 4	16.372%
Composite 3 & 7	21.360%	Composite 1 & 5	17.189%
Composite 3 & 9	21.834%	Composite 1 & 7	20.766%
Composite 3 & 10	23.758%	Composite 1 & 9	17.546%
Composite 3 & 11	22.786%	Composite 1 & 10	22.202%
Composite 3 & 15	25.547%	Composite 1 & 11	14.239%
Composite 3 & 16	26.219%	Composite 1 & 15	14.602%
Composite 3 & 17	25.567%	Composite 1 & 16	17.988%
Composite 3 & 19	23.931%	Composite 1 & 17	12.623%
Composite 3 & 20	26.713%	Composite 1 & 19	14.359%
Composite 4 & 5	19.302%	Composite 1 & 20	15.696%
Composite 4 & 7	22.844%		
Composite 4 & 9	20.190%		
Composite 4 & 10	22.689%		
Composite 4 & 11	17.011%		
Composite 4 & 15	17.830%		
Composite 4 & 16	20.989%		
Composite 4 & 17	17.072%		
Composite 4 & 19	16.851%		
Composite 4 & 20	22.493%		
Composite 5 & 7	23.773%		
Composite 5 & 9	18.050%		
Composite 5 & 10	24.411%		
Composite 5 & 11	19.414%		
Composite 5 & 15	20.232%		
Composite 5 & 16	23.958%		
Composite 5 & 17	17.793%		
Composite 5 & 19	17.161%		
Composite 5 & 20	22.451%		
Composite 7 & 9	21.132%		
Composite 7 & 10	26.480%		
Composite 7 & 11	22.153%		

Composite 7 & 15	23.270%
Composite 7 & 16	25.665%
Composite 7 & 17	22.224%
Composite 7 & 19	21.997%
Composite 7 & 20	24.794%
Composite 9 & 10	21.902%
Composite 9 & 11	19.725%
Composite 9 & 15	22.474%
Composite 9 & 16	21.070%
Composite 9 & 17	19.906%
Composite 9 & 19	18.836%
Composite 9 & 20	21.040%
Composite 10 & 11	24.036%
Composite 10 & 15	23.317%
Composite 10 & 16	24.808%
Composite 10 & 17	23.015%
Composite 10 & 19	21.795%
Composite 10 & 20	25.702%
Composite 11 & 15	19.927%
Composite 11 & 16	21.086%
Composite 11 & 17	19.523%
Composite 11 & 19	14.676%
Composite 11 & 20	18.412%
Composite 15 & 16	20.136%
Composite 15 & 17	18.143%
Composite 15 & 19	14.248%
Composite 15 & 20	17.201%
Composite 16 & 17	18.107%
Composite 16 & 19	15.046%
Composite 16 & 20	21.027%
Composite 17 & 19	14.391%
Composite 17 & 20	20.259%
Composite 19 & 20	19.005%

Difference between ‘control’ samples % Area and ‘field’ samples % Area, 3.722%.

‘Control’ samples 1, 4, 5, 7, 9, 10, 11, 15, 16, 17, 19, 20 and ‘field’ sample 3

‘Control’ Samples		**‘Field’ Sample**	
Image	**% Area**	**Image**	**% Area**
Composite 1 & 4	16.372%	Composite 3 & 1	25.139%
Composite 1 & 5	17.189%	Composite 3 & 4	24.784%
Composite 1 & 7	20.766%	Composite 3 & 5	20.119%
Composite 1 & 9	17.546%	Composite 3 & 7	21.360%
Composite 1 & 10	22.202%	Composite 3 & 9	21.834%
Composite 1 & 11	14.239%	Composite 3 & 10	23.758%
Composite 1 & 15	14.602%	Composite 3 & 11	22.786%
Composite 1 & 16	17.988%	Composite 3 & 15	25.547%
Composite 1 & 17	12.623%	Composite 3 & 16	26.219%
Composite 1 & 19	14.359%	Composite 3 & 17	25.567%
Composite 1 & 20	15.696%	Composite 3 & 19	23.931%
Composite 4 & 5	19.302%	Composite 3 & 20	26.713%
Composite 4 & 7	22.844%		
Composite 4 & 9	20.190%		
Composite 4 & 10	22.689%		
Composite 4 & 11	17.011%		
Composite 4 & 15	17.830%		
Composite 4 & 16	20.989%		
Composite 4 & 17	17.072%		
Composite 4 & 19	16.851%		
Composite 4 & 20	22.493%		
Composite 5 & 7	23.773%		
Composite 5 & 9	18.050%		
Composite 5 & 10	24.411%		
Composite 5 & 11	19.414%		
Composite 5 & 15	20.232%		
Composite 5 & 16	23.958%		
Composite 5 & 17	17.793%		
Composite 5 & 19	17.161%		
Composite 5 & 20	22.451%		
Composite 7 & 9	21.132%		
Composite 7 & 10	26.480%		
Composite 7 & 11	22.153%		
Composite 7 & 15	23.270%		
Composite 7 & 16	25.665%		

Composite 7 & 17	22.224%
Composite 7 & 19	21.997%
Composite 7 & 20	24.794%
Composite 9 & 10	21.902%
Composite 9 & 11	19.725%
Composite 9 & 15	22.474%
Composite 9 & 16	21.070%
Composite 9 & 17	19.906%
Composite 9 & 19	18.836%
Composite 9 & 20	21.040%
Composite 10 & 11	24.036%
Composite 10 & 15	23.317%
Composite 10 & 16	24.808%
Composite 10 & 17	23.015%
Composite 10 & 19	21.795%
Composite 10 & 20	25.702%
Composite 11 & 15	19.927%
Composite 11 & 16	21.086%
Composite 11 & 17	19.523%
Composite 11 & 19	14.676%
Composite 11 & 20	18.412%
Composite 15 & 16	20.136%
Composite 15 & 17	18.143%
Composite 15 & 19	14.248%
Composite 15 & 20	17.201%
Composite 16 & 17	18.107%
Composite 16 & 19	15.046%
Composite 16 & 20	21.027%
Composite 17 & 19	14.391%
Composite 17 & 20	20.259%
Composite 19 & 20	19.005%

Difference between ‘control’ samples % Area and ‘field’ samples % Area, -4.061%.

‘Control’ samples 1, 3, 5, 7, 9, 10, 11, 15, 16, 17, 19, 20 and ‘field’ sample 4

‘Control’ Samples		**‘Field’ Sample**	
Image	**% Area**	**Image**	**% Area**
Composite 1 & 3	25.139%	Composite 4 & 1	16.372%
Composite 1 & 5	17.189%	Composite 4 & 3	24.784%
Composite 1 & 7	20.766%	Composite 4 & 5	19.302%
Composite 1 & 9	17.546%	Composite 4 & 7	22.844%
Composite 1 & 10	22.202%	Composite 4 & 9	20.190%
Composite 1 & 11	14.239%	Composite 4 & 10	22.689%
Composite 1 & 15	14.602%	Composite 4 & 11	17.011%
Composite 1 & 16	17.988%	Composite 4 & 15	17.830%
Composite 1 & 17	12.623%	Composite 4 & 16	20.989%
Composite 1 & 19	14.359%	Composite 4 & 17	17.072%
Composite 1 & 20	15.696%	Composite 4 & 19	16.851%
Composite 3 & 5	20.119%	Composite 4 & 20	22.493%
Composite 3 & 7	21.360%		
Composite 3 & 9	21.834%		
Composite 3 & 10	23.758%		
Composite 3 & 11	22.786%		
Composite 3 & 15	25.547%		
Composite 3 & 16	26.219%		
Composite 3 & 17	25.567%		
Composite 3 & 19	23.931%		
Composite 3 & 20	26.713%		
Composite 5 & 7	23.773%		
Composite 5 & 9	18.050%		
Composite 5 & 10	24.411%		
Composite 5 & 11	19.414%		
Composite 5 & 15	20.232%		
Composite 5 & 16	23.958%		
Composite 5 & 17	17.793%		
Composite 5 & 19	17.161%		
Composite 5 & 20	22.451%		
Composite 7 & 9	21.132%		
Composite 7 & 10	26.480%		
Composite 7 & 11	22.153%		
Composite 7 & 15	23.270%		
Composite 7 & 16	25.665%		

Composite 7 & 17	22.224%
Composite 7 & 19	21.997%
Composite 7 & 20	24.794%
Composite 9 & 10	21.902%
Composite 9 & 11	19.725%
Composite 9 & 15	22.474%
Composite 9 & 16	21.070%
Composite 9 & 17	19.906%
Composite 9 & 19	18.836%
Composite 9 & 20	21.040%
Composite 10 & 11	24.036%
Composite 10 & 15	23.317%
Composite 10 & 16	24.808%
Composite 10 & 17	23.015%
Composite 10 & 19	21.795%
Composite 10 & 20	25.702%
Composite 11 & 15	19.927%
Composite 11 & 16	21.086%
Composite 11 & 17	19.523%
Composite 11 & 19	14.676%
Composite 11 & 20	18.412%
Composite 15 & 16	20.136%
Composite 15 & 17	18.143%
Composite 15 & 19	14.248%
Composite 15 & 20	17.201%
Composite 16 & 17	18.107%
Composite 16 & 19	15.046%
Composite 16 & 20	21.027%
Composite 17 & 19	14.391%
Composite 17 & 20	20.259%
Composite 19 & 20	19.005%

Difference between ‘control’ samples % Area and ‘field’ samples % Area, 0.797%.

‘Control’ samples 1, 3, 4, 7, 9, 10, 11, 15, 16, 17, 19, 20 and ‘field’ sample 5

‘Control’ Samples		**‘Field’ Sample**	
Image	**% Area**	**Image**	**% Area**
Composite 1 & 3	25.139%	Composite 5 & 1	17.189%
Composite 1 & 4	16.372%	Composite 5 & 3	20.119%
Composite 1 & 7	20.766%	Composite 5 & 4	19.302%
Composite 1 & 9	17.546%	Composite 5 & 7	23.773%
Composite 1 & 10	22.202%	Composite 5 & 9	18.050%
Composite 1 & 11	14.239%	Composite 5 & 10	24.411%
Composite 1 & 15	14.602%	Composite 5 & 11	19.414%
Composite 1 & 16	17.988%	Composite 5 & 15	20.232%
Composite 1 & 17	12.623%	Composite 5 & 16	23.958%
Composite 1 & 19	14.359%	Composite 5 & 17	17.793%
Composite 1 & 20	15.696%	Composite 5 & 19	17.161%
Composite 3 & 4	24.784%	Composite 5 & 20	22.451%
Composite 3 & 7	21.360%		
Composite 3 & 9	21.834%		
Composite 3 & 10	23.758%		
Composite 3 & 11	22.786%		
Composite 3 & 15	25.547%		
Composite 3 & 16	26.219%		
Composite 3 & 17	25.567%		
Composite 3 & 19	23.931%		
Composite 3 & 20	26.713%		
Composite 4 & 7	22.844%		
Composite 4 & 9	20.190%		
Composite 4 & 10	22.689%		
Composite 4 & 11	17.011%		
Composite 4 & 15	17.830%		
Composite 4 & 16	20.989%		
Composite 4 & 17	17.072%		
Composite 4 & 19	16.851%		
Composite 4 & 20	22.493%		
Composite 7 & 9	21.132%		
Composite 7 & 10	26.480%		
Composite 7 & 11	22.153%		
Composite 7 & 15	23.270%		
Composite 7 & 16	25.665%		

Composite 7 & 17	22.224%
Composite 7 & 19	21.997%
Composite 7 & 20	24.794%
Composite 9 & 10	21.902%
Composite 9 & 11	19.725%
Composite 9 & 15	22.474%
Composite 9 & 16	21.070%
Composite 9 & 17	19.906%
Composite 9 & 19	18.836%
Composite 9 & 20	21.040%
Composite 10 & 11	24.036%
Composite 10 & 15	23.317%
Composite 10 & 16	24.808%
Composite 10 & 17	23.015%
Composite 10 & 19	21.795%
Composite 10 & 20	25.702%
Composite 11 & 15	19.927%
Composite 11 & 16	21.086%
Composite 11 & 17	19.523%
Composite 11 & 19	14.676%
Composite 11 & 20	18.412%
Composite 15 & 16	20.136%
Composite 15 & 17	18.143%
Composite 15 & 19	14.248%
Composite 15 & 20	17.201%
Composite 16 & 17	18.107%
Composite 16 & 19	15.046%
Composite 16 & 20	21.027%
Composite 17 & 19	14.391%
Composite 17 & 20	20.259%
Composite 19 & 20	19.005%

Difference between ‘control’ samples % Area and ‘field’ samples % Area, 0.263%.

‘Control’ samples 1, 3, 4, 5, 9, 10, 11, 15, 16, 17, 19, 20 and ‘field’ sample 7

‘Control’ Samples		**‘Field’ Sample**	
Image	**% Area**	**Image**	**% Area**
Composite 1 & 3	25.139%	Composite 7 & 1	20.766%
Composite 1 & 4	16.372%	Composite 7 & 3	21.360%
Composite 1 & 5	17.189%	Composite 7 & 4	22.844%
Composite 1 & 9	17.546%	Composite 7 & 5	23.773%
Composite 1 & 10	22.202%	Composite 7 & 9	21.132%
Composite 1 & 11	14.239%	Composite 7 & 10	26.480%
Composite 1 & 15	14.602%	Composite 7 & 11	22.153%
Composite 1 & 16	17.988%	Composite 7 & 15	23.270%
Composite 1 & 17	12.623%	Composite 7 & 16	25.665%
Composite 1 & 19	14.359%	Composite 7 & 17	22.224%
Composite 1 & 20	15.696%	Composite 7 & 19	21.997%
Composite 3 & 4	24.784%	Composite 7 & 20	24.794%
Composite 3 & 5	20.119%		
Composite 3 & 9	21.834%		
Composite 3 & 10	23.758%		
Composite 3 & 11	22.786%		
Composite 3 & 15	25.547%		
Composite 3 & 16	26.219%		
Composite 3 & 17	25.567%		
Composite 3 & 19	23.931%		
Composite 3 & 20	26.713%		
Composite 4 & 5	19.302%		
Composite 4 & 9	20.190%		
Composite 4 & 10	22.689%		
Composite 4 & 11	17.011%		
Composite 4 & 15	17.830%		
Composite 4 & 16	20.989%		
Composite 4 & 17	17.072%		
Composite 4 & 19	16.851%		
Composite 4 & 20	22.493%		
Composite 5 & 9	18.050%		
Composite 5 & 10	24.411%		
Composite 5 & 11	19.414%		
Composite 5 & 15	20.323%		
Composite 5 & 16	23.958%		

Composite 5 & 17	17.793%
Composite 5 & 19	17.161%
Composite 5 & 20	22.451%
Composite 9 & 10	21.902%
Composite 9 & 11	19.725%
Composite 9 & 15	22.474%
Composite 9 & 16	21.070%
Composite 9 & 17	19.906%
Composite 9 & 19	18.836%
Composite 9 & 20	21.040%
Composite 10 & 11	24.036%
Composite 10 & 15	23.317%
Composite 10 & 16	24.808%
Composite 10 & 17	23.015%
Composite 10 & 19	21.795%
Composite 10 & 20	25.702%
Composite 11 & 15	19.927%
Composite 11 & 16	21.086%
Composite 11 & 17	19.523%
Composite 11 & 19	14.676%
Composite 11 & 20	18.412%
Composite 15 & 16	20.136%
Composite 15 & 17	18.143%
Composite 15 & 19	14.248%
Composite 15 & 20	17.201%
Composite 16 & 17	18.107%
Composite 16 & 19	15.046%
Composite 16 & 20	21.027%
Composite 17 & 19	14.391%
Composite 17 & 20	20.259%
Composite 19 & 20	19.005%

Difference between ‘control’ samples % Area and ‘field’ samples % Area, -2.948%.

‘Control’ samples 1, 3, 4, 5, 7, 10, 11, 15, 16, 17, 19, 20 and ‘field’ sample 9

‘Control’ Samples		**‘Field’ Sample**	
Image	**% Area**	**Image**	**% Area**
Composite 1 & 3	25.139%	Composite 9 & 1	17.546%
Composite 1 & 4	16.372%	Composite 9 & 3	21.834%
Composite 1 & 5	17.189%	Composite 9 & 4	20.190%
Composite 1 & 7	20.766%	Composite 9 & 5	18.050%
Composite 1 & 10	22.202%	Composite 9 & 7	21.132%
Composite 1 & 11	14.239%	Composite 9 & 10	21.902%
Composite 1 & 15	14.602%	Composite 9 & 11	19.725%
Composite 1 & 16	17.988%	Composite 9 & 15	22.474%
Composite 1 & 17	12.623%	Composite 9 & 16	21.070%
Composite 1 & 19	14.359%	Composite 9 & 17	19.906%
Composite 1 & 20	15.696%	Composite 9 & 19	18.836%
Composite 3 & 4	24.784%	Composite 9 & 20	21.040%
Composite 3 & 5	20.119%		
Composite 3 & 7	21.360%		
Composite 3 & 10	23.758%		
Composite 3 & 11	22.786%		
Composite 3 & 15	25.547%		
Composite 3 & 16	26.219%		
Composite 3 & 17	25.567%		
Composite 3 & 19	23.931%		
Composite 3 & 20	26.713%		
Composite 4 & 5	19.302%		
Composite 4 & 7	22.844%		
Composite 4 & 10	22.689%		
Composite 4 & 11	17.011%		
Composite 4 & 15	17.830%		
Composite 4 & 16	20.989%		
Composite 4 & 17	17.072%		
Composite 4 & 19	16.851%		
Composite 4 & 20	22.493%		
Composite 5 & 7	23.773%		
Composite 5 & 10	24.411%		
Composite 5 & 11	19.414%		
Composite 5 & 15	20.323%		
Composite 5 & 16	23.958%		

Composite 5 & 17	17.793%
Composite 5 & 19	17.161%
Composite 5 & 20	22.451%
Composite 7 & 10	26.480%
Composite 7 & 11	22.153%
Composite 7 & 15	23.270%
Composite 7 & 16	25.665%
Composite 7 & 17	22.224%
Composite 7 & 19	21.997%
Composite 7 & 20	24.794%
Composite 10 & 11	24.036%
Composite 10 & 15	23.317%
Composite 10 & 16	24.808%
Composite 10 & 17	23.015%
Composite 10 & 19	21.795%
Composite 10 & 20	25.702%
Composite 11 & 15	19.927%
Composite 11 & 16	21.086%
Composite 11 & 17	19.523%
Composite 11 & 19	14.676%
Composite 11 & 20	18.412%
Composite 15 & 16	20.136%
Composite 15 & 17	18.143%
Composite 15 & 19	14.248%
Composite 15 & 20	17.201%
Composite 16 & 17	18.107%
Composite 16 & 19	15.046%
Composite 16 & 20	21.027%
Composite 17 & 19	14.391%
Composite 17 & 20	20.259%
Composite 19 & 20	19.005%

Difference between ‘control’ samples % Area and ‘field’ samples % Area, 0.277%.

‘Control’ samples 1, 3, 4, 5, 7, 9, 11, 15, 16, 17, 19, 20 and ‘field’ sample 10

Composite 1 & 3	25.139%	Composite 10 & 1	22.202%
Composite 1 & 4	16.372%	Composite 10 & 3	23.758%
Composite 1 & 5	17.189%	Composite 10 & 4	22.689%
Composite 1 & 7	20.766%	Composite 10 & 5	24.411%
Composite 1 & 9	17.546%	Composite 10 & 7	26.480%
Composite 1 & 11	14.239%	Composite 10 & 9	21.902%
Composite 1 & 15	14.602%	Composite 10 & 11	24.036%
Composite 1 & 16	17.988%	Composite 10 & 15	23.317%
Composite 1 & 17	12.623%	Composite 10 & 16	24.808%
Composite 1 & 19	14.359%	Composite 10 & 17	23.015%
Composite 1 & 20	15.696%	Composite 10 & 19	21.795%
Composite 3 & 4	24.784%	Composite 10 & 20	25.702%
Composite 3 & 5	20.119%		
Composite 3 & 7	21.360%		
Composite 3 & 9	21.834%		
Composite 3 & 11	22.786%		
Composite 3 & 15	25.547%		
Composite 3 & 16	26.219%		
Composite 3 & 17	25.567%		
Composite 3 & 19	23.931%		
Composite 3 & 20	26.713%		
Composite 4 & 5	19.302%		
Composite 4 & 7	22.844%		
Composite 4 & 9	20.190%		
Composite 4 & 11	17.011%		
Composite 4 & 15	17.830%		
Composite 4 & 16	20.989%		
Composite 4 & 17	17.072%		
Composite 4 & 19	16.851%		
Composite 4 & 20	22.493%		
Composite 5 & 7	23.773%		
Composite 5 & 9	18.050%		
Composite 5 & 11	19.414%		
Composite 5 & 15	20.232%		
Composite 5 & 16	23.958%		
Composite 5 & 17	17.793%		
Composite 5 & 19	17.161%		

Composite 5 & 20	22.451%
Composite 7 & 9	21.132%
Composite 7 & 11	22.153%
Composite 7 & 15	23.270%
Composite 7 & 16	25.665%
Composite 7 & 17	22.224%
Composite 7 & 19	21.997%
Composite 7 & 20	24.794%
Composite 9 & 11	19.725%
Composite 9 & 15	22.474%
Composite 9 & 16	21.070%
Composite 9 & 17	19.906%
Composite 9 & 19	18.836%
Composite 9 & 20	21.040%
Composite 11 & 15	19.927%
Composite 11 & 16	21.086%
Composite 11 & 17	19.523%
Composite 11 & 19	14.676%
Composite 11 & 20	18.412%
Composite 15 & 16	20.136%
Composite 15 & 17	18.143%
Composite 15 & 19	14.248%
Composite 15 & 20	17.201%
Composite 16 & 17	18.107%
Composite 16 & 19	15.046%
Composite 16 & 20	21.027%
Composite 17 & 19	14.391%
Composite 17 & 20	20.259%
Composite 19 & 20	19.005%

Difference between ‘control’ samples % Area and ‘field’ samples % Area, -3.702%.

‘Control’ samples 1, 3, 4, 5, 7, 9, 10, 15, 16, 17, 19, 20 and ‘field’ sample 11

Composite 1 & 3	25.139%	Composite 11 & 1	14.239%
Composite 1 & 4	16.372%	Composite 11 & 3	22.786%
Composite 1 & 5	17.189%	Composite 11 & 4	17.011%
Composite 1 & 7	20.766%	Composite 11 & 5	19.414%
Composite 1 & 9	17.546%	Composite 11 & 7	22.153%
Composite 1 & 10	22.202%	Composite 11 & 9	19.725%
Composite 1 & 15	14.602%	Composite 11 & 10	24.036%
Composite 1 & 16	17.988%	Composite 11 & 15	19.927%
Composite 1 & 17	12.623%	Composite 11 & 16	21.086%
Composite 1 & 19	14.359%	Composite 11 & 17	19.523%
Composite 1 & 20	15.696%	Composite 11 & 19	14.676%
Composite 3 & 4	24.784%	Composite 11 & 20	18.412%
Composite 3 & 5	20.119%		
Composite 3 & 7	21.360%		
Composite 3 & 9	21.834%		
Composite 3 & 10	23.758%		
Composite 3 & 15	25.547%		
Composite 3 & 16	26.219%		
Composite 3 & 17	25.567%		
Composite 3 & 19	23.931%		
Composite 3 & 20	26.713%		
Composite 4 & 5	19.302%		
Composite 4 & 7	22.844%		
Composite 4 & 9	20.190%		
Composite 4 & 10	22.689%		
Composite 4 & 15	17.830%		
Composite 4 & 16	20.989%		
Composite 4 & 17	17.072%		
Composite 4 & 19	16.851%		
Composite 4 & 20	22.493%		
Composite 5 & 7	23.773%		
Composite 5 & 9	18.050%		
Composite 5 & 10	24.411%		
Composite 5 & 15	20.232%		
Composite 5 & 16	23.958%		
Composite 5 & 17	17.793%		
Composite 5 & 19	17.161%		

Composite 5 & 20	22.451%
Composite 7 & 9	21.132%
Composite 7 & 10	26.480%
Composite 7 & 15	23.270%
Composite 7 & 16	25.665%
Composite 7 & 17	22.224%
Composite 7 & 19	21.997%
Composite 7 & 20	24.794%
Composite 9 & 10	21.902%
Composite 9 & 15	22.474%
Composite 9 & 16	21.070%
Composite 9 & 17	19.906%
Composite 9 & 19	18.836%
Composite 9 & 20	21.040%
Composite 10 & 15	23.317%
Composite 10 & 16	24.808%
Composite 10 & 17	23.015%
Composite 10 & 19	21.795%
Composite 10 & 20	25.702%
Composite 15 & 16	20.136%
Composite 15 & 17	18.143%
Composite 15 & 19	14.248%
Composite 15 & 20	17.201%
Composite 16 & 17	18.107%
Composite 16 & 19	15.046%
Composite 16 & 20	21.027%
Composite 17 & 19	14.391%
Composite 17 & 20	20.259%
Composite 19 & 20	19.005%

Difference between ‘control’ samples % Area and ‘field’ samples % Area, 1.333%.

‘Control’ samples 1, 3, 4, 5, 7, 9, 10, 11, 16, 17, 19, 20 and ‘field’ sample 15

Composite 1 & 3	25.139%	Composite 15 & 1	14.602%
Composite 1 & 4	16.372%	Composite 15 & 3	25.547%
Composite 1 & 5	17.189%	Composite 15 & 4	17.830%
Composite 1 & 7	20.766%	Composite 15 & 5	20.232%
Composite 1 & 9	17.546%	Composite 15 & 7	23.270%
Composite 1 & 10	22.202%	Composite 15 & 9	22.474%
Composite 1 & 11	14.239%	Composite 15 & 10	23.317%
Composite 1 & 16	17.988%	Composite 15 & 11	19.927%
Composite 1 & 17	12.623%	Composite 15 & 16	20.136%
Composite 1 & 19	14.359%	Composite 15 & 17	18.143%
Composite 1 & 20	15.696%	Composite 15 & 19	14.248%
Composite 3 & 4	24.784%	Composite 15 & 20	17.201%
Composite 3 & 5	20.119%		
Composite 3 & 7	21.360%		
Composite 3 & 9	21.834%		
Composite 3 & 10	23.758%		
Composite 3 & 11	22.786%		
Composite 3 & 16	26.219%		
Composite 3 & 17	25.567%		
Composite 3 & 19	23.931%		
Composite 3 & 20	26.713%		
Composite 4 & 5	19.302%		
Composite 4 & 7	22.844%		
Composite 4 & 9	20.190%		
Composite 4 & 10	22.689%		
Composite 4 & 11	17.011%		
Composite 4 & 16	20.989%		
Composite 4 & 17	17.072%		
Composite 4 & 19	16.851%		
Composite 4 & 20	22.493%		
Composite 5 & 7	23.773%		
Composite 5 & 9	18.050%		
Composite 5 & 10	24.411%		
Composite 5 & 11	19.414%		
Composite 5 & 16	23.958%		
Composite 5 & 17	17.793%		
Composite 5 & 19	17.161%		

Composite 5 & 20	22.451%
Composite 7 & 9	21.132%
Composite 7 & 10	26.480%
Composite 7 & 11	22.153%
Composite 7 & 16	25.665%
Composite 7 & 17	22.224%
Composite 7 & 19	21.997%
Composite 7 & 20	24.794%
Composite 9 & 10	21.902%
Composite 9 & 11	19.725%
Composite 9 & 16	21.070%
Composite 9 & 17	19.906%
Composite 9 & 19	18.836%
Composite 9 & 20	21.040%
Composite 10 & 11	24.036%
Composite 10 & 16	24.808%
Composite 10 & 17	23.015%
Composite 10 & 19	21.795%
Composite 10 & 20	25.702%
Composite 11 & 16	21.086%
Composite 11 & 17	19.523%
Composite 11 & 19	14.676%
Composite 11 & 20	18.412%
Composite 16 & 17	18.107%
Composite 16 & 19	15.046%
Composite 16 & 20	21.027%
Composite 17 & 19	14.391%
Composite 17 & 20	20.259%
Composite 19 & 20	19.005%

Difference between ‘control’ samples % Area and ‘field’ samples % Area, 0.945%.

‘Control’ samples 1, 3, 4, 5, 7, 9, 10, 11, 15, 17, 19, 20 and ‘field’ sample 16

Composite 1 & 3	25.139%	Composite 16 & 1	17.988%
Composite 1 & 4	16.372%	Composite 16 & 3	26.219%
Composite 1 & 5	17.189%	Composite 16 & 4	20.989%
Composite 1 & 7	20.766%	Composite 16 & 5	23.958%
Composite 1 & 9	17.546%	Composite 16 & 7	25.665%
Composite 1 & 10	22.202%	Composite 16 & 9	21.070%
Composite 1 & 11	14.239%	Composite 16 & 10	24.808%
Composite 1 & 15	14.602%	Composite 16 & 11	21.086%
Composite 1 & 17	12.623%	Composite 16 & 15	20.136%
Composite 1 & 19	14.359%	Composite 16 & 17	18.107%
Composite 1 & 20	15.696%	Composite 16 & 19	15.046%
Composite 3 & 4	24.784%	Composite 16 & 20	21.027%
Composite 3 & 5	20.119%		
Composite 3 & 7	21.360%		
Composite 3 & 9	21.834%		
Composite 3 & 10	23.758%		
Composite 3 & 11	22.786%		
Composite 3 & 15	25.547%		
Composite 3 & 17	25.567%		
Composite 3 & 19	23.931%		
Composite 3 & 20	26.713%		
Composite 4 & 5	19.302%		
Composite 4 & 7	22.844%		
Composite 4 & 9	20.190%		
Composite 4 & 10	22.689%		
Composite 4 & 11	17.011%		
Composite 4 & 15	17.830%		
Composite 4 & 17	17.072%		
Composite 4 & 19	16.851%		
Composite 4 & 20	22.493%		
Composite 5 & 7	23.773%		
Composite 5 & 9	18.050%		
Composite 5 & 10	24.411%		
Composite 5 & 11	19.414%		
Composite 5 & 15	20.232%		
Composite 5 & 17	17.793%		
Composite 5 & 19	17.161%		

Composite 5 & 20	22.451%
Composite 7 & 9	21.132%
Composite 7 & 10	26.480%
Composite 7 & 11	22.153%
Composite 7 & 15	23.270%
Composite 7 & 17	22.224%
Composite 7 & 19	21.997%
Composite 7 & 20	24.794%
Composite 9 & 10	21.902%
Composite 9 & 11	19.725%
Composite 9 & 15	22.474%
Composite 9 & 17	19.906%
Composite 9 & 19	18.836%
Composite 9 & 20	21.040%
Composite 10 & 11	24.036%
Composite 10 & 15	23.317%
Composite 10 & 17	23.015%
Composite 10 & 19	21.795%
Composite 10 & 20	25.702%
Composite 11 & 15	19.927%
Composite 11 & 17	19.523%
Composite 11 & 19	14.676%
Composite 11 & 20	18.412%
Composite 15 & 17	18.143%
Composite 15 & 19	14.248%
Composite 15 & 20	20.259%
Composite 17 & 19	14.391%
Composite 17 & 20	20.259%
Composite 19 & 20	19.005%

Difference between ‘control’ samples % Area and ‘field’ samples % Area, -0.943%.

‘Control’ samples 1, 3, 4, 5, 7, 9, 10, 11, 15, 16, 19, 20 and ‘field’ sample 17

Composite 1 & 3	25.139%	Composite 17 & 1	12.623%
Composite 1 & 4	16.372%	Composite 17 & 3	25.567%
Composite 1 & 5	17.189%	Composite 17 & 4	17.072%
Composite 1 & 7	20.766%	Composite 17 & 5	17.793%
Composite 1 & 9	17.546%	Composite 17 & 7	22.224%
Composite 1 & 10	22.202%	Composite 17 & 9	19.906%
Composite 1 & 11	14.239%	Composite 17 & 10	23.015%
Composite 1 & 15	14.602%	Composite 17 & 11	19.523%
Composite 1 & 16	17.988%	Composite 17 & 15	18.143%
Composite 1 & 19	14.359%	Composite 17 & 16	18.107%
Composite 1 & 20	15.696%	Composite 17 & 19	14.391%
Composite 3 & 4	24.784%	Composite 17 & 20	20.259%
Composite 3 & 5	20.119%		
Composite 3 & 7	21.360%		
Composite 3 & 9	21.834%		
Composite 3 & 10	23.758%		
Composite 3 & 11	22.786%		
Composite 3 & 15	25.547%		
Composite 3 & 16	26.219%		
Composite 3 & 19	23.931%		
Composite 3 & 20	26.713%		
Composite 4 & 5	19.302%		
Composite 4 & 7	22.844%		
Composite 4 & 9	20.190%		
Composite 4 & 10	22.689%		
Composite 4 & 11	17.011%		
Composite 4 & 15	17.830%		
Composite 4 & 16	20.989%		
Composite 4 & 19	16.851%		
Composite 4 & 20	22.493%		
Composite 5 & 7	23.773%		
Composite 5 & 9	18.050%		
Composite 5 & 10	24.411%		
Composite 5 & 11	19.414%		
Composite 5 & 15	20.232%		
Composite 5 & 16	23.958%		
Composite 5 & 19	17.161%		

Composite 5 & 20	22.451%
Composite 7 & 9	21.132%
Composite 7 & 10	26.480%
Composite 7 & 11	22.153%
Composite 7 & 15	23.270%
Composite 7 & 16	25.665%
Composite 7 & 19	21.997%
Composite 7 & 20	24.794%
Composite 9 & 10	21.902%
Composite 9 & 11	19.725%
Composite 9 & 15	22.474%
Composite 9 & 16	21.070%
Composite 9 & 19	18.836%
Composite 9 & 20	21.040%
Composite 10 & 11	24.036%
Composite 10 & 15	23.317%
Composite 10 & 16	24.808%
Composite 10 & 19	21.795%
Composite 10 & 20	25.702%
Composite 11 & 15	19.927%
Composite 11 & 16	21.086%
Composite 11 & 19	14.676%
Composite 11 & 20	18.412%
Composite 15 & 16	20.136%
Composite 15 & 19	14.248%
Composite 15 & 20	20.259%
Composite 16 & 19	15.046%
Composite 16 & 20	21.027%
Composite 19 & 20	19.005%

Difference between ‘control’ samples % Area and ‘field’ samples % Area, 1.763%.

‘Control’ samples 1, 3, 4, 5, 7, 9, 10, 11, 15, 16, 17, 20 and ‘field’ sample 19

Composite 1 & 3	25.139%	Composite 19 & 1	14.359%
Composite 1 & 4	16.372%	Composite 19 & 3	23.931%
Composite 1 & 5	17.189%	Composite 19 & 4	16.851%
Composite 1 & 7	20.766%	Composite 19 & 5	17.161%
Composite 1 & 9	17.546%	Composite 19 & 7	21.997%
Composite 1 & 10	22.202%	Composite 19 & 9	18.836%
Composite 1 & 11	14.239%	Composite 19 & 10	21.795%
Composite 1 & 15	14.602%	Composite 19 & 11	14.676%
Composite 1 & 16	17.988%	Composite 19 & 15	14.248%
Composite 1 & 17	12.623%	Composite 19 & 16	15.046%
Composite 1 & 20	15.696%	Composite 19 & 17	14.391%
Composite 3 & 4	24.784%	Composite 19 & 20	19.005%
Composite 3 & 5	20.119%		
Composite 3 & 7	21.360%		
Composite 3 & 9	21.834%		
Composite 3 & 10	23.758%		
Composite 3 & 11	22.786%		
Composite 3 & 15	25.547%		
Composite 3 & 16	26.219%		
Composite 3 & 17	25.567%		
Composite 3 & 20	26.713%		
Composite 4 & 5	19.302%		
Composite 4 & 7	22.844%		
Composite 4 & 9	20.190%		
Composite 4 & 10	22.689%		
Composite 4 & 11	17.011%		
Composite 4 & 15	17.830%		
Composite 4 & 16	20.989%		
Composite 4 & 17	17.072%		
Composite 4 & 20	22.493%		
Composite 5 & 7	23.773%		
Composite 5 & 9	18.050%		
Composite 5 & 10	24.411%		
Composite 5 & 11	19.414%		
Composite 5 & 15	20.232%		
Composite 5 & 16	23.958%		
Composite 5 & 17	17.793%		

Composite 5 & 20	22.451%
Composite 7 & 9	21.132%
Composite 7 & 10	26.480%
Composite 7 & 11	22.153%
Composite 7 & 15	23.270%
Composite 7 & 16	25.665%
Composite 7 & 17	22.224%
Composite 7 & 20	24.794%
Composite 9 & 10	21.902%
Composite 9 & 11	19.725%
Composite 9 & 15	22.474%
Composite 9 & 16	21.070%
Composite 9 & 17	19.906%
Composite 9 & 20	21.040%
Composite 10 & 11	24.036%
Composite 10 & 15	23.317%
Composite 10 & 16	24.808%
Composite 10 & 17	23.015%
Composite 10 & 20	25.702%
Composite 11 & 15	19.927%
Composite 11 & 16	21.086%
Composite 11 & 17	19.523%
Composite 11 & 20	18.412%
Composite 15 & 16	20.136%
Composite 15 & 17	18.143%
Composite 15 & 20	20.259%
Composite 16 & 17	18.107%
Composite 16 & 20	21.027%
Composite 17 & 20	20.259%

Difference between ‘control’ samples % Area and ‘field’ samples % Area, 3.371%.

‘Control’ samples 1, 3, 4, 5, 7, 9, 10, 11, 15, 16, 17, 19, and ‘field’ sample 20

Composite 1 & 3	25.139%	Composite 20 & 1	15.696%
Composite 1 & 4	16.372%	Composite 20 & 3	26.713%
Composite 1 & 5	17.189%	Composite 20 & 4	22.493%
Composite 1 & 7	20.766%	Composite 20 & 5	22.451%
Composite 1 & 9	17.546%	Composite 20 & 7	24.794%
Composite 1 & 10	22.202%	Composite 20 & 9	21.040%
Composite 1 & 11	14.239%	Composite 20 & 10	25.702%
Composite 1 & 15	14.602%	Composite 20 & 11	18.412%
Composite 1 & 16	17.988%	Composite 20 & 15	17.201%
Composite 1 & 17	12.623%	Composite 20 & 16	21.027%
Composite 1 & 19	14.359%	Composite 20 & 17	20.259%
Composite 3 & 4	24.784%	Composite 20 & 19	19.005%
Composite 3 & 5	20.119%		
Composite 3 & 7	21.360%		
Composite 3 & 9	21.834%		
Composite 3 & 10	23.758%		
Composite 3 & 11	22.786%		
Composite 3 & 15	25.547%		
Composite 3 & 16	26.219%		
Composite 3 & 17	25.567%		
Composite 3 & 19	23.931%		
Composite 4 & 5	19.302%		
Composite 4 & 7	22.844%		
Composite 4 & 9	20.190%		
Composite 4 & 10	22.689%		
Composite 4 & 11	17.011%		
Composite 4 & 15	17.830%		
Composite 4 & 16	20.989%		
Composite 4 & 17	17.072%		
Composite 4 & 19	16.851%		
Composite 5 & 7	23.773%		
Composite 5 & 9	18.050%		
Composite 5 & 10	24.411%		
Composite 5 & 11	19.414%		
Composite 5 & 15	20.232%		
Composite 5 & 16	23.958%		
Composite 5 & 17	17.793%		

Composite 5 & 19	17.161%
Composite 7 & 9	21.132%
Composite 7 & 10	26.480%
Composite 7 & 11	22.153%
Composite 7 & 15	23.270%
Composite 7 & 16	25.665%
Composite 7 & 17	22.224%
Composite 7 & 19	21.997%
Composite 9 & 10	21.902%
Composite 9 & 11	19.725%
Composite 9 & 15	22.474%
Composite 9 & 16	21.070%
Composite 9 & 17	19.906%
Composite 9 & 19	18.836%
Composite 10 & 11	24.036%
Composite 10 & 15	23.317%
Composite 10 & 16	24.808%
Composite 10 & 17	23.015%
Composite 10 & 19	21.795%
Composite 11 & 15	19.927%
Composite 11 & 16	21.086%
Composite 11 & 17	19.523%
Composite 11 & 19	14.676%
Composite 15 & 16	20.136%
Composite 15 & 17	18.143%
Composite 15 & 19	14.248%
Composite 16 & 17	18.107%
Composite 16 & 19	15.046%
Composite 17 & 19	14.391%

Difference between ‘control’ samples % Area and ‘field’ samples % Area, -1.043%.

VITA

Name: Roushan Ghanbari

Address: Texas A&M University Department of Nuclear Engineering
322 Teague Research Center
Texas A&M University
College Station, TX 77843

Email Address: Roushan.Ghanbari@gmail.com

Education: B.S., Mechanical Engineering, New Mexico Institute of Mining and Technology, 2009

M.S., Nuclear Engineering, Texas A&M University, 2011